Australian Synchrotron
Research Highlights 2007 - 2009

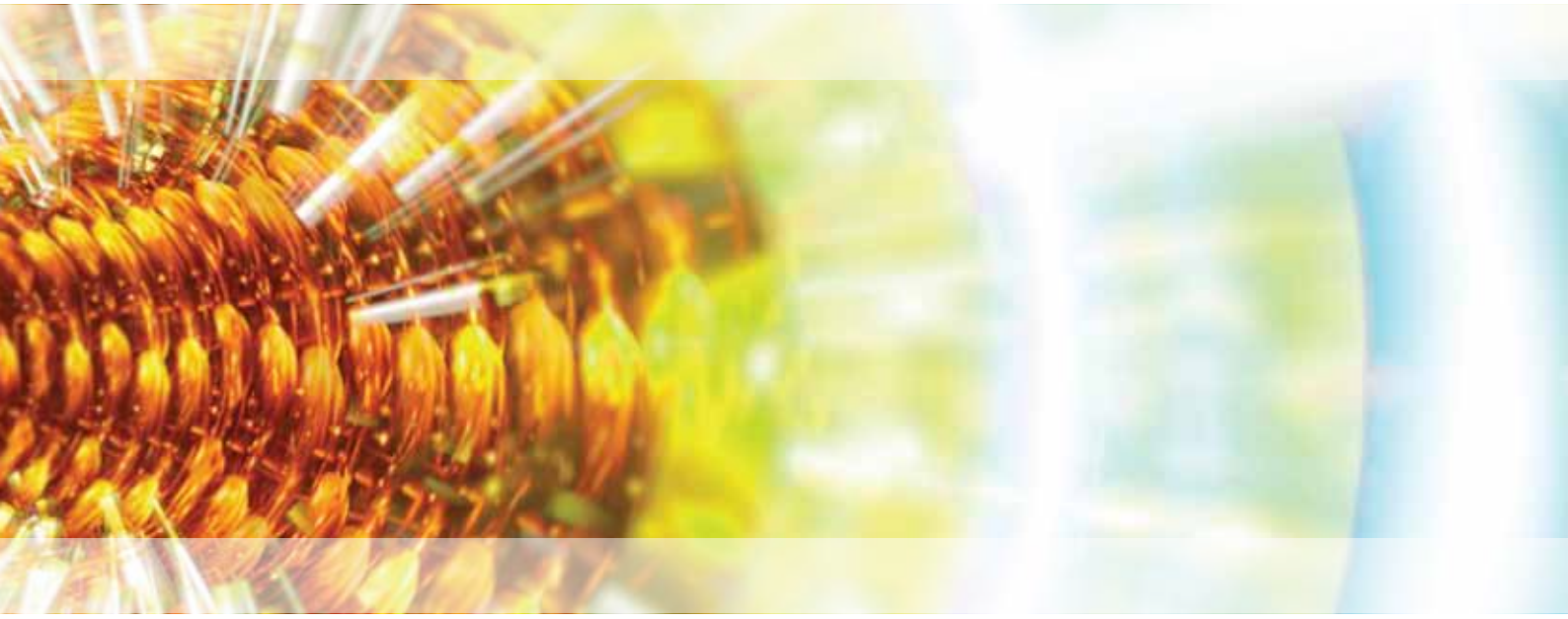

Australian Synchrotron

Supported by

Australian Government

State Government Victoria AUSTRALIA

Contents

Cover Image: 'Lightbridge ' by Chris Henschke

Melbourne based digital artist Chris Henschke undertook a residency at the Australian Synchrotron funded through the Arts Victoria Arts Innovation program and the Australian Network for Art and Technology in 2007. During his stay he used the Australian Synchrotron to collect visual data. One visualisation experiment produced the image used on the cover of this report. Chris is now undertaking a second artistic residency at the Australian Synchrotron also funded by the Australian Network for Art and Technology.

Foreword

During my tenure as Head of Science at the Australian Synchrotron, I was fortunate to oversee a period of rapid growth in capability and outcomes.

Accordingly, I am pleased to announce the publication of the Australian Synchrotron's first Research Highlights Report.

This report covers the period from the Australian Synchrotron's opening in June 2007 to the end of 2009 and provides a short description of the facility, a summary of its capabilities and scientific highlights, its publications and presentations, information about our users, details of the process for applying for beam time and information about our foundation investors.

As a state-of-the-art, 3 GeV light source, the Australian Synchrotron has nine beamlines allowing experiments to be performed in a wide variety of scientific fields from macromolecular and micro-crystallography, powder diffraction and x-ray fluorescence microscopy to infrared spectroscopy.

Synchrotron techniques like these and others open up critical new possibilities in understanding the molecular structure, properties and nature of materials, and how they change, react and interact with one another, providing sectors such as agriculture, advanced materials, food sciences, mining, micro-technology and pharmaceuticals with new and innovative research methods; methods that deliver cheaper and sometimes faster scientific results.

In recognising the significant developments that have occurred over the 2007 to 2009 period, it is important we acknowledge the vision and tireless work of a number of groups who were instrumental in establishing this facility.

Without the work and dedication of those at the Australian National Beamline Facility (ANBF, Tsukuba, Japan 1991-1995), individuals involved in the Australian Synchrotron Research Program (ASRP, 1995-2008) and the critical support offered by Foundation Investors, this facility would not be a reality today.

We would like to thank these groups, the State Government of Victoria, the Australian Federal Government and the New Zealand Government for their continued support of this state-of-the-art research facility.

I believe this report provides a robust record of the Australian Synchrotron's development and major achievements; achievements that validate the support given by the facility's funders and Foundation Investors.

Since its inception, the facility has had over 2000 users pass through its doors and seen over 200 research papers published. In addition, four thousand people have visited the facility under its combined marketing and education and outreach programs.

In its relatively short life, the Australian Synchrotron has already made a vital contribution to numerous high-profile research projects, raising and bolstering the image of the nation's university and research sectors, while also improving the economic and social welfare of all Australians.

"In its relatively short life, the AS has already made a vital contribution to numerous high-profile research projects, raising and bolstering the image of the nation's university and research sectors, while also improving the economic and social welfare of all Australians."

While the state and federal governments actively review the Australian Synchrotron's second investment and science case, detailing the rationale for, and benefits of, increasing the number of beamlines at the facility, the Australian Synchrotron is moving forward with its existing plans for expansion and growth.

These plans will focus on the construction of several new buildings including a National Centre for Synchrotron Science, the construction of a new user accommodation centre, development of an office extension building and completion of a technical support laboratory.

The Australian Synchrotron believes these plans and the creation of further beamlines at the facility will make a positive contribution to the development of stronger research outcomes into the future; outcomes that will continue to place the Australian Synchrotron at the forefront of scientific research and development.

We hope you enjoy reading the Australian Synchrotron's first Research Highlights Report.

Professor Ian Gentle

(Professor Ian Gentle was Head of Science at the Australian Synchrotron from October 2008 - December 2010)

The Australian Synchrotron

About us

As a third-generation, 3 GeV light source, the Australian Synchrotron is a leading science and research facility supporting a diverse and exciting mix of scientific and commercial research activities.

Since its opening in June 2007, the facility and its scientists have established nine beamlines offering users a range of scientific techniques from powder diffraction and macro-molecular crystallography to x-ray absorption spectroscopy.

Using this range of non-destructive, high-resolution, rapid, in-situ, real-time imaging and analysis techniques, which are far superior in accuracy, clarity, specificity and timeliness to conventional laboratory equipment, users can now better understand at a molecular level, the structure, shape and function of substances and the way they change, react and interact with one another.

In its short life, the Australian Synchrotron has already achieved significant research outcomes. These include providing a unique insight into the conditions underlying sensory perception and the analysis of solar wind samples from the NASA Genesis spacecraft. The facility has also made notable contributions to the development of new treatments aiding cancer, mental illness, IVF and malaria.

Today, use of synchrotron science is considered an essential element in the development of many knowledge-intensive industries, including biotechnology and nanotechnology, and other more traditional industries such as pharmaceuticals, mining and telecommunications.

The Australian Synchrotron is funded by the Victorian State Government, the Australian Federal Government, the New Zealand Government and a number of national and international science-based consortia.

Its vision is to be the catalyst for the best scientific research and innovation in Australasia, with its focus to provide a thriving scientific research environment conducive to creating and nurturing the best scientific outcomes for users and staff of the facility.

Capabilities

Accelerator Science and Operations

The heart of the Australian Synchrotron is its light source, the 'machine' that generates synchrotron x-rays and infrared light for diverse research experiments. The major components of the synchrotron light source include an electron gun, which generates a stream of electrons, and a linear accelerator, which accelerates the electrons until they are moving at close to light speed. Next the electrons are accelerated to their operating energy in the booster ring. The final stage is the storage ring, where the electron beam (made up of electron bunches approximately 60 centimetres apart) circulates for many hours, producing 'synchrotron light' that is harvested for use in experiments.

The light source is operated and maintained by a highly trained team working in close collaboration with other specialists who conduct research aimed at improving the characteristics of the light source – and the quality of the light generated for use in beamline experiments.

The Imaging and Medical beamline

When completed in 2012, the Imaging and Medical beamline will provide unrivalled x-ray imaging and radiotherapy capabilities for a wide range of research applications from medicine to specialised materials research. It will deliver a wide x-ray beam by 4 cm x-ray beam to a satellite building that is fully equipped for pre-clinical and clinical research.

The extended beamline and satellite building facility currently under construction will provide high-resolution imaging of cells, tissues and tumours, enable cell tracking using markers, and facilitate radiotherapy research. The beamline's cardiac and cardiovascular, lung and tissue (breasts, bones and organs) imaging capabilities will also allow preclinical programs to be extended to clinical research with patients.

The Infrared beamlines

The Australian Synchrotron has two infrared beamlines that are operated independently. One is used for infrared microspectroscopy, the other for far-infrared and high-resolution infrared studies.

Infrared spectroscopy is widely used in research, analytical and industrial laboratories. The synchrotron infrared microspectroscopy beamline extends the scope of this popular technique, and can locate and analyse individual components in samples with dimensions of only a few microns, producing high spatial resolution chemical images.

The far-infrared and high-resolution infrared beamline offers high spectral resolution infrared spectroscopy for characterising gas phase samples, solids and thin films on surfaces.

The Macromolecular Crystallography beamlines

Macromolecular crystallography is the study of the structure of large biomolecules such as proteins and nucleic acids using x-ray crystallography. Proteins are essential to life and carry out almost all reactions inside living cells.

X-ray diffraction is the most widely-used method for protein structure determination, providing essential information for a wide range of applications, including drug development, food technology, agriculture, manufacturing and chemical processing.

Determining the structures of proteins provides valuable information on how these "molecular machines" work, how they evolved and how to design drugs to modify their actions. This information can be used to design specific drugs that target proteins involved in diseases such as cancer, HIV, tuberculosis and malaria.

The Australian Synchrotron has two crystallography beamlines. The macromolecular crystallography (MX1) beamline is a high-throughput beamline for users with large numbers of samples. The micro-crystallography (MX2) beamline also caters for difficult crystals that are small or weakly diffracting. Remote access is available on both beamlines by prior arrangement.

The Powder Diffraction beamline

Powder Diffraction provides information on the crystal structure of polycrystalline natural and synthetic materials that can be related to the properties of those materials. It permits the study of bulk materials and provides a robust alternative for structural characterisation when single crystals are not available, as is often the case in nature and the laboratory.

Applications include in-situ studies of reaction mechanisms, investigations of crystal chemistry, phase identification and determination of how crystal structure affects physical, chemical or magnetic properties. The technique is used for studying a wide variety of samples and processes, including pharmaceuticals, radioactive waste materials, battery components such as electrolytes and electrodes, mineral ores and mineral processing conditions.

Compared to conventional laboratory-based powder diffraction, synchrotron powder diffraction offers superior, more accurate data, excellent signal-to-noise outcomes, faster time-frames and can be used to examine significantly smaller samples. A further advantage is that synchrotron x-rays can be tuned to particular wavelengths to suit sample composition and experimental requirements.

The Small and Wide Angle x-ray Scattering beamline

The Small and Wide Angle x-ray Scattering beamline provides information on the structure of materials on scales ranging from atomic to molecular to particle scale: from 1 angstrom up to 400 nanometres. Many types of materials have structure on the nano scale, including liquid emulsions, colloids, particles, proteins and surfaces.

SAXS provides useful structural information on a wide range of solids, powders, gels, liquids and solutions, including biological materials, polymers, coatings, biosensors, and mineral ores and products. The technique is a valuable complement to x-ray crystallographic structural determinations.

The beamline also offers simultaneous WAXS, which is useful for structures ranging down to the atomic level. The beamline's WAXS capabilities are used for projects such as phase analysis in minerals, molecular packing in polymers, and small-scale structures in surfactants. In many cases, the SAXS and WAXS measurements are taken simultaneously to study dynamics at differing scales.

The Soft x-ray Spectroscopy beamline

This beamline can provide information on bond lengths, coordination numbers, coordination geometry and oxidation state for atoms with atomic numbers below 20 (hydrogen to calcium) for a wide range of solid and liquid samples.

It is mainly used for near-edge x-ray absorption fine structure (NEXAFS) studies. NEXAFS can only be done at synchrotrons because it requires the ability to scan through a range of x-ray energies. The beamline also offers soft x-ray photoelectron spectroscopy (SXPS), which gives higher photon resolution and sensitivity than conventional laboratory XPS.

The x-ray Absorption Spectroscopy beamline

X-ray Absorption Spectroscopy techniques provide chemical and structural information on atoms from calcium to uranium for a wide range of solid and liquid systems. XAS experiments require an intense, tuneable photon source only available at synchrotrons.

The x-ray absorption near-edge structure (XANES) region of an XAS spectrum yields chemical information such as local coordination geometry and oxidation state. The extended x-ray absorption fine structure (EXAFS) region provides structural information such as bond length, coordination number and disorder.

Widely used by both specialists and non-specialists, XAS is a mature technology that enables the advancement of new areas of science. The technique complements protein crystallography studies, and the two are frequently used in combination to determine challenging structures.

The x-ray Fluorescence Microscopy beamline

The x-ray Fluorescence Microscopy beamline provides valuable elemental, structural and chemical information from a very diverse range of samples with micrometre and sub-micrometre resolution (less than one-hundredth the width of a human hair).

XFM produces a detailed x-ray image of a whole sample by collecting data from small sections and combining these to make up the full picture. It can simultaneously identify the presence and determine the level in the sample of multiple elements such as iron, magnesium, copper and gold. The technique is particularly useful in biology, geology and mining, environmental studies and forensics. The beamline's nanoprobe capabilities can resolve features as small as 200 nanometres, making it ideal for sub-cellular elemental mapping and imaging of biological samples.

International Synchrotron Access Program (ISAP)

From 2009 ISAP supported 71 visits to overseas synchrotron facilities. This program is managed by the Australian Synchrotron.

Australian National Beam line Facility (ANBF)

Between September 2008 and 2009, the ANBF and its funding program (which has been managed by the Australian Synchrotron since mid 2008) supported 52 visits by Australian-based groups to the Japanese facility.

Highlights

This section contains highlights selected from all the Australian Synchrotron-related peer-reviewed journal articles, published conference proceedings, conference papers, book chapters and theses published between July 2007, when researchers officially began using the Australian Synchrotron to further their research goals, and December 2009. All these publications draw on data obtained at the Australian Synchrotron, the Australian National Beamline Facility or other overseas facilities with financial support from the Australian Synchrotron Research Program or the International Synchrotron Access Program or which list Australian Synchrotron staff members as authors.

Research typically involves a lengthy journey from ideas, concepts and theories to experiments, results and conclusions, and from there to further experimentation or development. Major research programs can take many years to reach their final goals. Along the way, the findings are published whenever the researchers have something of particular value to report to their peers.

The highlights presented in this report demonstrate the high quality of the research conducted at or supported by the Australian Synchrotron in the early years of a facility that is designed to continue operating for decades to come. This impressive early output augurs well for the Australian Synchrotron's ability to provide ongoing benefits for the Australian and New Zealand scientific and industrial research and development communities.

- High-resolution details of long, thin, protein assemblies called pili that enable diphtheria-causing bacteria to attach to host tissues offer fresh insights into bacterial evolution and potential routes to new vaccines.

- Nanostructured materials that self-assemble are increasingly being used in applications such as drug delivery, and providing new insights into cellular processes involving lipid bilayer membranes in living organisms.

- Researchers are using synchrotron techniques to gradually build a detailed picture of our highly complex immune system.
    - A newly identified mechanism that the immune system uses to maintain self-tolerance highlights the versatility of the T cell repertoire and interaction with peptide-MHC complexes.
    - Structural studies of natural killer T-cell receptors have revealed greater scope for differential recognition of a broad variety of lipid-based antigens.
    - The finding that induced-fit molecular mimicry underpins T-cell alloreactions has implications for reducing morbidity and mortality rates associated with tissue transplantation.

- Synchrotron Fourier transform infrared studies have paved the way for development of an automated infrared-based technology capable of diagnosing malaria at all stages of the parasite's lifecycle inside red blood cells.

- Close examination of the structure and chemical states of nitrogen atoms in nitrogen-doped zinc oxide films suggests that specific annealing temperatures are required for creation of p-type semiconductor zinc oxide films, which could potentially be used in many optoelectronic applications.

- The Maia detector array has demonstrated megapixel high-definition trace element imaging on the x-ray fluorescence microscopy (XFM) beamline at the Australian Synchrotron, with faster acquisition and improved counting statistics.

- Powder diffraction is an invaluable tool for conducting parametric studies of perovskite structures, providing an overview of form and function that is important for harnessing the useful electronic and magnetic properties of these versatile materials. Researchers recently investigated a series of doped perovskite manganites with varying ratios of strontium, calcium and neodymium.

- A promising new approach to stabilising electron beams combines feedback control with neural network feed-forward techniques. Developed at the Australian Synchrotron as part of an international project, the new system will help ensure the best possible light quality at next-generation light sources.

- In the period 2007 – 2009, access to the Australian Synchrotron (AS), ISAP (International Synchrotron Access Program) and ASRP (Australian Synchrotron Research Program) resulted in 422 papers being published in journals across the world. This activity was made possible through direct funding from the Australian Government.

- Access to overseas facilities during this period was administered under three programs: the ASRP (managed by ANSTO), which ended in July 2008, the ISAP and the Australian National Beamline Facility access program.

New details of key bacterial structures involved in diphtherial infections

The *Corynebacterium diphtheriae* shaft pilin SpaA is built of tandem Ig-like modules with stabilising isopeptide and disulfide bonds

H.J. Kang, N.G. Paterson, A.H. Gaspar, H. Ton-That, and E.N. Baker, The *Corynebacterium diphtheriae* shaft pilin SpaA is built of tandem Ig-like modules with stabilizing isopeptide and disulfide bonds, P. Natl. Acad. Sci. U.S.A., 106, 16967-16971, (2009). Impact factor 9.432.

High-resolution details of long, thin, protein assemblies called pili that enable diphtheria-causing bacteria to attach to host tissues offer fresh insights into bacterial evolution and potential routes to new vaccines.

Diphtheria is a potentially fatal bacterial disease that affects the upper respiratory tract. In most industrialised countries, including Australia, the disease has largely been eradicated through large-scale vaccination programs. However, it still claims lives in other parts of the world, and can be fatal in as many as one in five cases.

The causative agent, *Corynebacterium diphtheriae*, has long, hairlike, protein assemblies called pili on its cell surface that enable it to infect its human host. These very thin structures were first observed in 2003 by one of this paper's co-authors. Remarkably, they had been unknown until then. Their discovery and characterisation as covalent polymers was a milestone in understanding colonisation and infection by Gram-positive bacteria.

Bacterial pili have aroused great interest because of their direct roles in infection and pathogenesis and their importance as vaccine candidates. What is remarkable about the pili from *Corynebacterium diphtheriae* is that they use covalent isopeptide (amide) bonds, both intermolecular and intramolecular, for strength and stability, and thus present a new paradigm among protein polymers. Isopeptide bonds are like the bonds that join amino acids together in a protein backbone chain, but it is highly unusual for an isopeptide bond to occur as an internal crosslink between side chains.

Using the MX2 beamline at the Australian Synchrotron, a collaborative NZ-US research team has now obtained a high-resolution (1.6 angstroms) crystal structure of SpaA, the protein that forms the polymeric shaft of the *C. diphtheriae* pilus.

The *C. diphtheriae* SpaA shaft pilin consists of three immunoglobulin-like domains, arranged like beads on a string. Two of these domains contain isopeptide bond crosslinks formed between lysine and asparagine side chains. The bonds form when the protein folds as the lysine–asparagine pair is brought together in a hydrophobic environment. One domain of SpaA also contains a disulfide bond.

The two internal isopeptide bonds in SpaA resemble those found previously in pili from another pathogenic bacterium, *Streptococcus pyogenes*, which causes sore throats and tonsillitis as well as severe invasive illnesses such as rheumatic fever. They have since also been found in the bacteria that cause pneumococcal disease and anthrax.

The results reported in this paper reveal that despite profound dissimilarities in primary sequences, the shaft pilins of Gram-positive pathogens have strikingly similar tertiary structures. This suggests a likely common architecture for the backbones of many Gram-positive pili involving modular construction and stabilising intermolecular and intramolecular isopeptide bonds.

The widespread occurrence of internal isopeptide crosslinks in the cell-surface proteins of Gram-positive bacteria indicates their structural and functional importance in enhancing thermodynamic stability and resistance to proteolysis. The strategic locations of the isopeptide bonds also impart mechanical (force-bearing) stability.

The disulfide bond in SpaA is not found in the pili of other Gram-positive bacteria, many of which lack the machinery to make disulfide bonds. This leads to the intriguing idea that isopeptide bonds may have evolved as an alternative means of stabilisation. Amide bonds are less prone to chemical disruption than disulfide bonds, which may be important for such thin, exposed assemblies.

Intriguingly, the SpaA molecules pack end-to-end in columns through the crystal, providing a very convincing model for the way they assemble into the actual pilus structure – a nice example of the way in which crystal structures can give quite unexpected insights into biological assemblies.

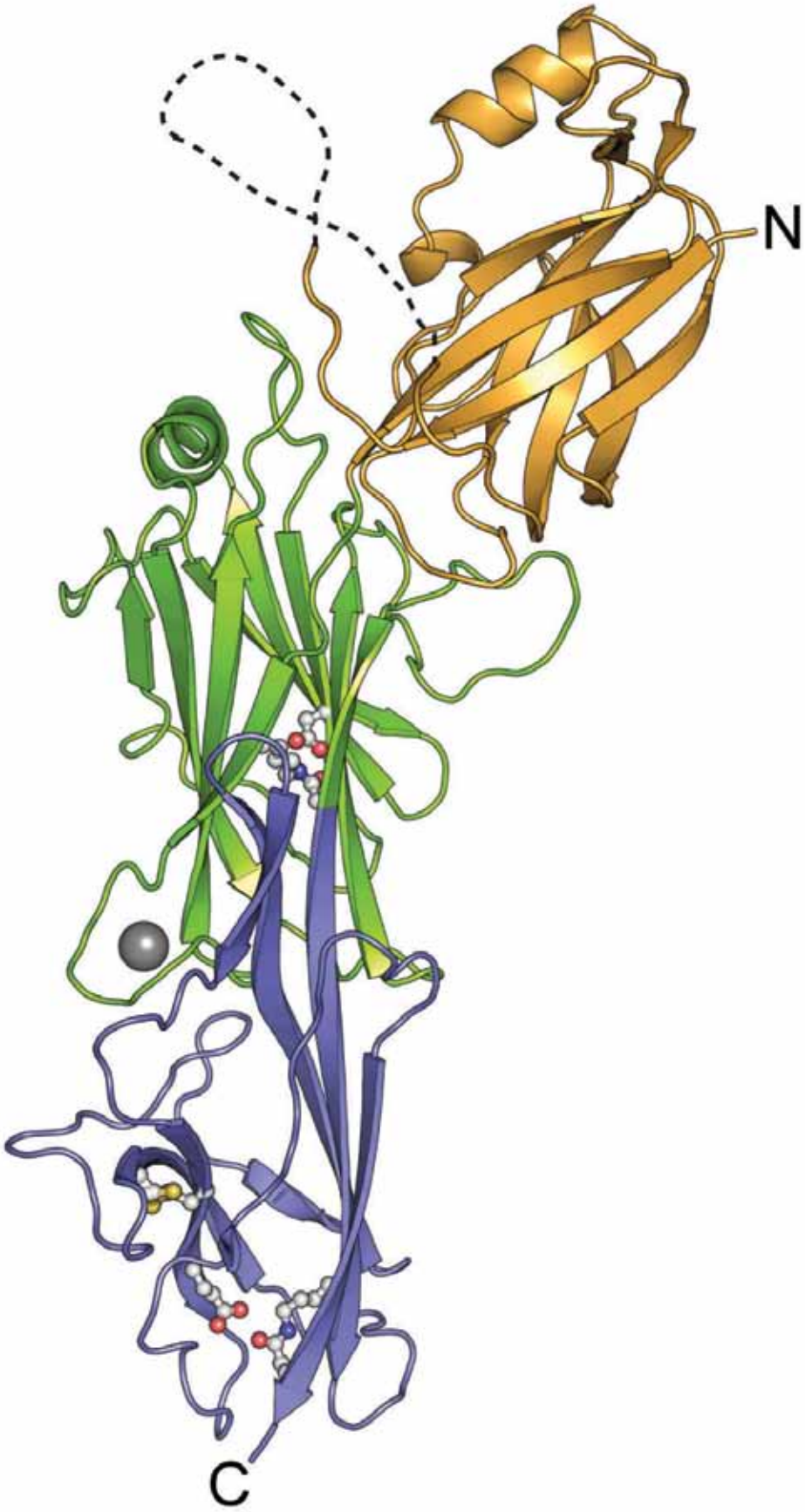

High resolution structure of the SpaA pilin protein from Corynebacterium diphtheriae. *Image: Edward Baker*

Self-assembled lipid nanoparticles

Observing self-assembled lipid nanoparticles building order and complexity through low-energy transformation processes

X. Mulet, X. Gong, L.J. Waddington, C.J. Drummond, Observing Self-Assembled Lipid Nanoparticles Building Order and Complexity through Low-Energy Transformation Processes, ACS Nano, 3 (9), 2789-2797 (2009). Impact factor 7.493.

Nanostructured materials that self-assemble are increasingly being used in applications such as drug delivery, and providing new insights into cellular processes involving lipid bilayer membranes in living organisms.

Nanostructured high surface area self-assembly materials are used for an increasing range of applications, including drug delivery, material templating, and membrane protein crystallography. Additionally, nanostructures of cubic symmetry occur in many cellular organelles, such as the endoplasmic reticulum and mitochondrial inner membranes. Complex 3D membrane reorganisation processes have been observed during skin barrier morphogenesis, and the transition from lamellar phase to cubic phase is considered a valuable model for biomembrane lipid scaffold remodelling events such as endocytosis.

Researchers from CSIRO Materials Science and Engineering believe the future of nanoscale soft matter design will be driven by the biological paradigms of hierarchical self-assembly and long-lived non-equilibrium states. Our ability to reproducibly control the low-energy self-assembly of nanomaterials will depend on our understanding of the highly ordered cubic membrane structures found in cellular organelles.

Developing a better understanding of how lipids build structural order and complexity is a key element in progressing bottom-up nanofabrication processes based on amphiphile self-assembly. However, a dynamic, non-equilibrium transition is by its very nature difficult to observe. It shows little order, cannot be resolved by standard x-ray diffraction techniques, and cannot be directly imaged owing to its short lifetime.

In 2009, Xavier Mulet and his colleagues from CSIRO and the University of Sydney used the small angle x-ray scattering (SAXS) beamline at the Australian Synchrotron in conjunction with cryo-transmission electron microscopy to successfully investigate the complete sequence of major transformations in the conversion from a one-dimensional lamellar membrane (L_α) to a three-dimensional inverse bicontinuous cubic nanostructure (Q_{II}^D).

The researchers used the two complementary techniques to observe and characterise initial lipid bilayer contacts and stalk formation followed by membrane pore development, pore evolution into 2D hexagonally-packed lattices, and finally the creation of 3D bicontinuous cubic structures.

The results indicate that stalk formation is a continuous process with constant changes in the curvature of the membrane system. Progression to a cubic phase lattice involves the formation of pores (interlamellar attachments or ILAs), which start to pack in a lowest energy configuration while maintaining preferential curvature in either a cubic or a hexagonal lattice. These lattices eventually stack into a close-packed hexagonal or close-packed cubic lattice that is a precursor to an intermediate mesophase known as phase X, itself a precursor to the cubic phase. Using a triblock copolymer to stabilise a highly-hydrated and relatively long-lived metastable phase, the researchers were able to conclude that this metastable phase was in fact the elusive phase X. The high degree of hydration enables the system to achieve the reduced pore size and decreased interpore distance required for ideal curvature configuration.

On the basis of their results, the researchers proposed a comprehensive model for cubic phase formation from a lamellar phase (the L_α to Q_{II}^D phase transition) involving: membrane undulations, stalk formation, interlamellar attachments (ILAs) via hemifusion rupture, ILA alignment and reduction in size, phase X formation, and formation of cubic lattice via swollen intermediate.

In a cell biology context, experimental confirmation of the intermediate lipid self-assembly structures advances our understanding of organelle morphogenesis and maturation as well as dynamic processes such as endocytosis and exocytosis. Cells may use similar steric effects, using membrane proteins for example, to control shape changes in membranes and mechanically affect rates of membrane reconfiguration.

The manipulation of intermediate structures such as ILAs in nanoparticulate dispersions of lipid self-assembly phases may provide a unique system for encapsulation and controlled release of bioactives. The ability to control intermediate transformations may also allow the development of flexible growth media for applications such as growing crystals of integral membrane proteins or liquid crystal templating of nanostructured materials. A better understanding of how amphiphiles use low-energy transformation processes to order and build complex structures will assist the creation of novel high-performance functional amphiphile self-assembly materials.

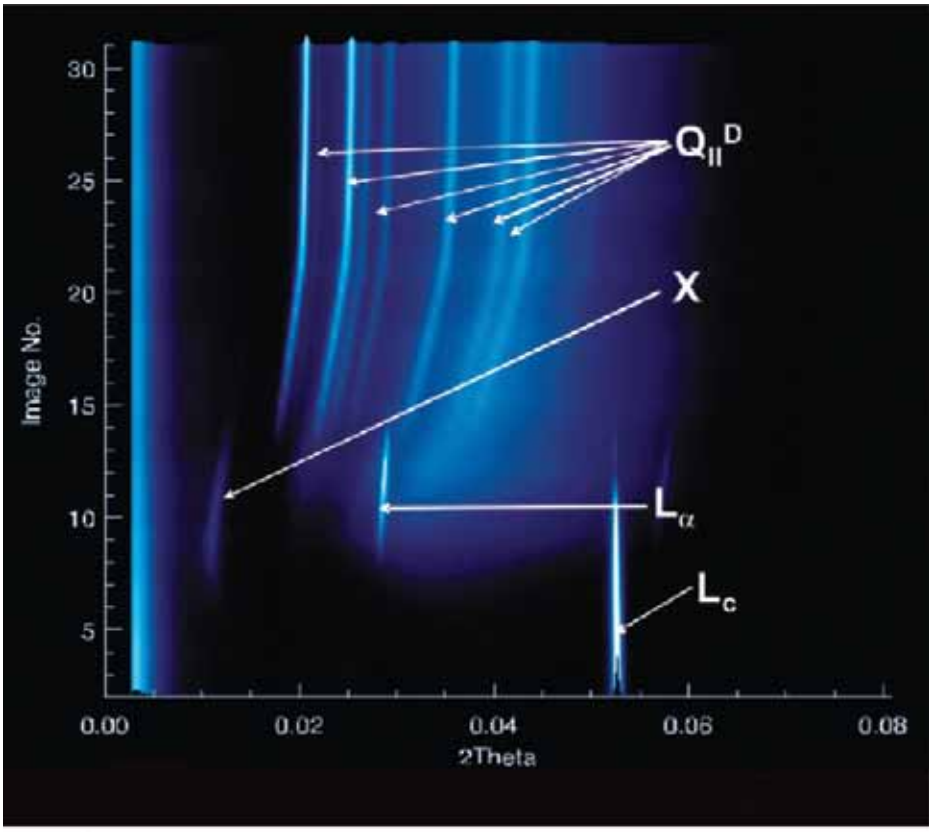

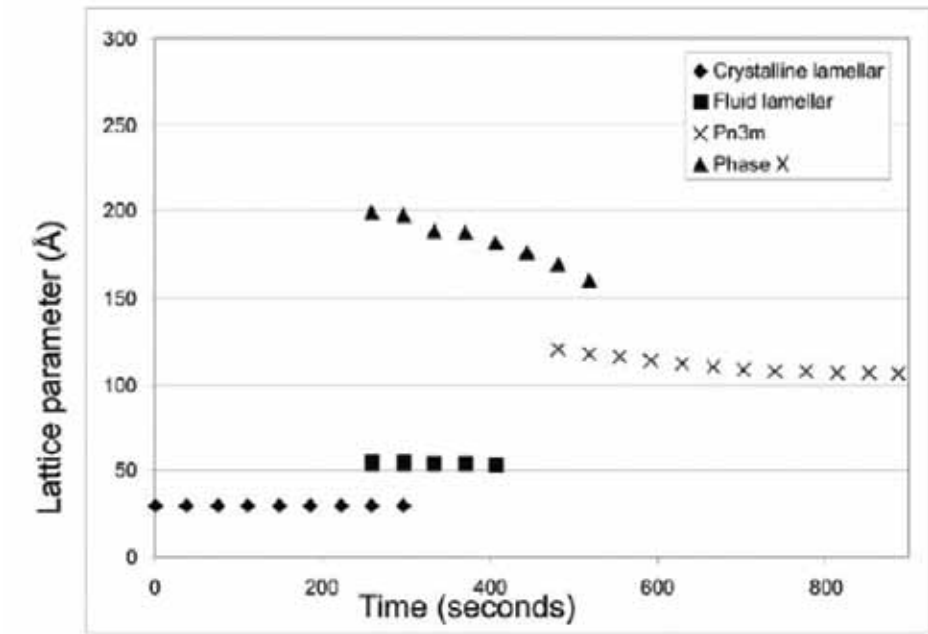

Synchrotron SAXS integrated diffraction patterns for a novel amphiphile pro-drug showing phase transitions from lamellar crystalline (L_c) to fluid lamellar (L_α) to double-diamond cubic nanostructure (Q_{II}^{D}). The elusive intermediate phase is marked 'X'. Image: Xavier Mulet and Calum Drummond, CSIRO

Understanding immune receptor function at the atomic level

In 2009, James McCluskey and Dale Godfrey from the University of Melbourne, Scott Burrows from Queensland Institute of Medical Research and Jamie Rossjohn from Monash University, their teams and collaborators published three Immunity papers (impact factor > 20) that drew on protein x-ray crystallography data collected at the Australian Synchrotron. The papers reported new advances in our understanding of T cells, a key component of the immune system, and have significant implications for immune-related disorders such as T-cell mediated transplant rejection.

The work is supported by grants and fellowships from the Australian Research Council, National Health and Medical Research Council and the ARC Centre of Excellence in Structural Functional Microbial Genomics.

Understanding immune receptor function at the atomic level (1)

The shaping of T cell receptor recognition by self-tolerance

S. Gras, S.R. Burrows, L. Kjer-Nielsen, C.S. Clements, Y.C. Liu, L.C. Sullivan, M.J. Bell, A.G. Brooks, A.W. Purcell, J. McCluskey and J. Rossjohn, Immunity 30, 193–203, February 20, 2009

A newly-identified mechanism that the immune system uses to maintain self-tolerance highlights the versatility of the T cell repertoire and interaction with peptide-MHC complexes.

How does the host avoid alloreactivity, and what are the mechanisms underpinning self-tolerance? This study addresses the central – but not well-understood – issue of how the immune system navigates the subtle distinction between self-restriction and self-tolerance.

This paper describes how self-tolerance toward a trans-HLA allotype shapes TCR recognition of an Epstein-Barr virus determinant (FLRGRAYGL). The researchers compared how HLA-B8-FLRGRAYGL is recognised by two archetypal TCRs: LC13 and CF34. In HLA B8+B44+ individuals, LC13 T-cells exhibit alloreactivity to HLA B44 and are therefore deleted from the repertoire. In those individuals, a new T-cell repertoire is generated against HLA B8-FLR to keep EBV in check; these new TCRs, which include CF34, lack HLA-B44 reactivity.

Both TCRs engaged the HLA B8-FLRGRAYGL equally effectively – but with markedly contrasting footprints. While the alloreactive LC13 TCR docked at the C terminus of HLA-B8-FLRGRAYGL, the CF34 TCR docked at the N terminus, creating potentially unfavourable interactions predicted to prevent cross-reaction with HLA-B44.

These findings simultaneously demonstrate a mechanism for avoiding autoreactivity and highlight the versatility of the T-cell repertoire and TCR interaction with peptide-MHC complexes.

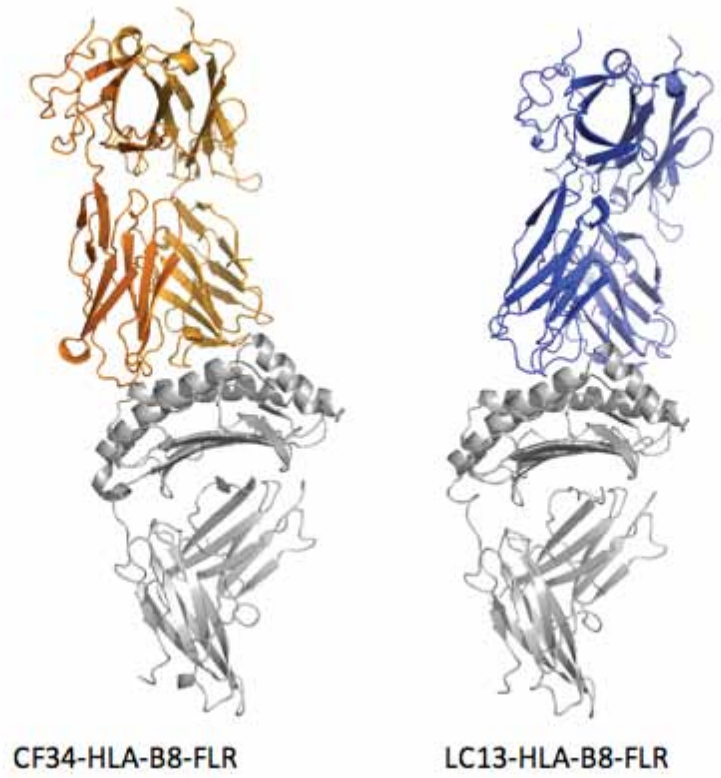

The docking mechanisms that T-cell receptors use to engage with target antigens can change to avoid autoreactivity.
Image: Jamie Rossjohn, Monash University

Understanding immune receptor function at the atomic level (2)

Differential recognition of CD1d-α-galactosyl ceramide by the Vß8.2 and Vß7 semi-invariant NKT T cell receptors

D.G. Pellicci, O. Patel, L. Kjer-Nielsen, S.S. Pang, L.C. Sullivan, K. Kyparissoudis, A.G. Brooks, H.H. Reid, S. Gras, I.S. Lucet, R. Koh, M.J. Smyth, T. Mallevaey, J.L. Matsuda, L. Gapin, J. McCluskey, D.I. Godfrey and J. Rossjohn, Immunity 31, 47–59, July 17, 2009

Structural studies of natural killer T-cell receptors have revealed greater scope for differential recognition of a broad variety of lipid-based antigens.

While MHC molecules present peptide antigens to T-cells, CD1d presents lipid-based antigens to natural killer T (NKT) cells. NKT cells are implicated in a broad range of diseases, including microbial immunity, tumour immunity, autoimmunity and allergy.

NKT cells in mice and humans typically express a semi-invariant T-cell receptor that pairs an invariant TCRα chain with a limited selection of TCRβ chains (Vβ11 in humans; Vβ8.2, Vβ7 and Vβ2 in mice). The TCRβ chains are important in determining the ability of NKT cells to recognise a large array of CD1d-restricted lipid antigens, including bacterial lipid, human self antigen like iGb3 or GD3.

This paper reports the structures of the Vβ8.2 and Vβ7 NKT TCRs in complex with mouse CD1d-α-galactosyl ceramide and compares them with a new higher-resolution structure of the human Vβ11 CD1d-α-GalCer.

The different NKT TCRβ chains converged on a common CD1d-antigen footprint, but with differences that partly reflect sequence and structural differences between the Vβ domains. Similarities between the homologous human Vβ11 and mouse Vβ8.2 domains highlight the conserved nature of this interaction across the 70 million years of evolution that separate mice and humans.

The results confirm that NKT TCR could be considered as a pattern recognition receptor, but also reveal the potential for greater diversity at the NKT TCR-CD1d interface – providing greater scope for differential recognition of a broad variety of CD1d-restricted antigens.

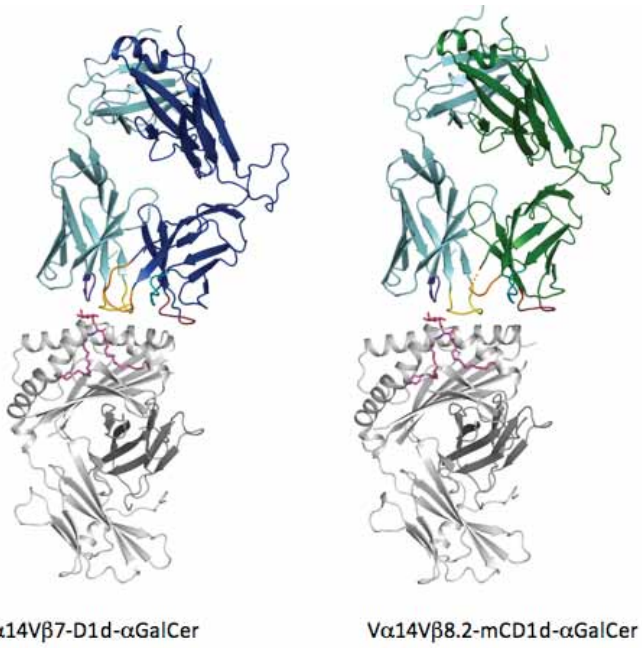

Recent studies have revealed how natural killer T (NKT) cells recognise lipid-based antigens and demonstrated their potential to recognise a broad range of antigens. Image: Jamie Rossjohn, Monash University

Understanding immune receptor function at the atomic level (3)

T cell allorecognition via molecular mimicry

W.A. Macdonald, Z. Chen, S. Gras, J.K. Archbold, F.E. Tynan, C.S. Clements, M. Bharadwaj, L. Kjer-Nielsen, P.M. Saunders, M.C.J. Wilce, F. Crawford, B. Stadinsky, D. Jackson, A.G. Brooks, A.W. Purcell, J.W. Kappler, S.R. Burrows, J. Rossjohn and J. McCluskey, Immunity 31, 897–908, December 18, 2009

The finding that induced-fit molecular mimicry underpins T-cell alloreactions has implications for reducing morbidity and mortality rates associated with tissue transplantation.

Mature T cells are restricted to recognising antigens presented by host MHC molecules, or self-MHC. However, some T cells are able to break the MHC-restriction law and can react with non-self MHC molecules; this is known as alloreactivity.

T cell alloreactivity with foreign human leukocyte antigens (HLAs) is responsible for much of the morbidity and mortality associated with tissue transplantation. However, despite its great clinical importance, the paradox of alloreactivity has remained a mystery for more than three decades.

This paper reports how the LC13 T-cell receptor (TCR) selected for recognition on self-HLA-B*0801 bound to a viral protein alloreacts with B44 allotypes (HLA-B*4402 and HLA-B*4405) bound to two different allopeptides. Despite extensive polymorphism between the three HLAs and differences in the viral and allopeptide sequences, the LC13 TCR engaged all three peptide-HLA (pHLA) complexes identically, accommodating mimicry of the viral peptide by the allopeptides.

The data presented in this paper highlight the intricate peptide dependence of T cell alloreactivity and show that direct T cell alloreactivity is attributable to exquisite TCR specificity rather than degenerate recognition of MHC. The findings suggest that in transplantation, nonpermissive taboo mismatches might depend on serendipitous mimicry that is lacking in permissive mismatches.

The authors suggest that mimicry will underpin most alloreactions, but note that more definitive data will be required regarding the relative roles of mimicry versus disparate docking modes.

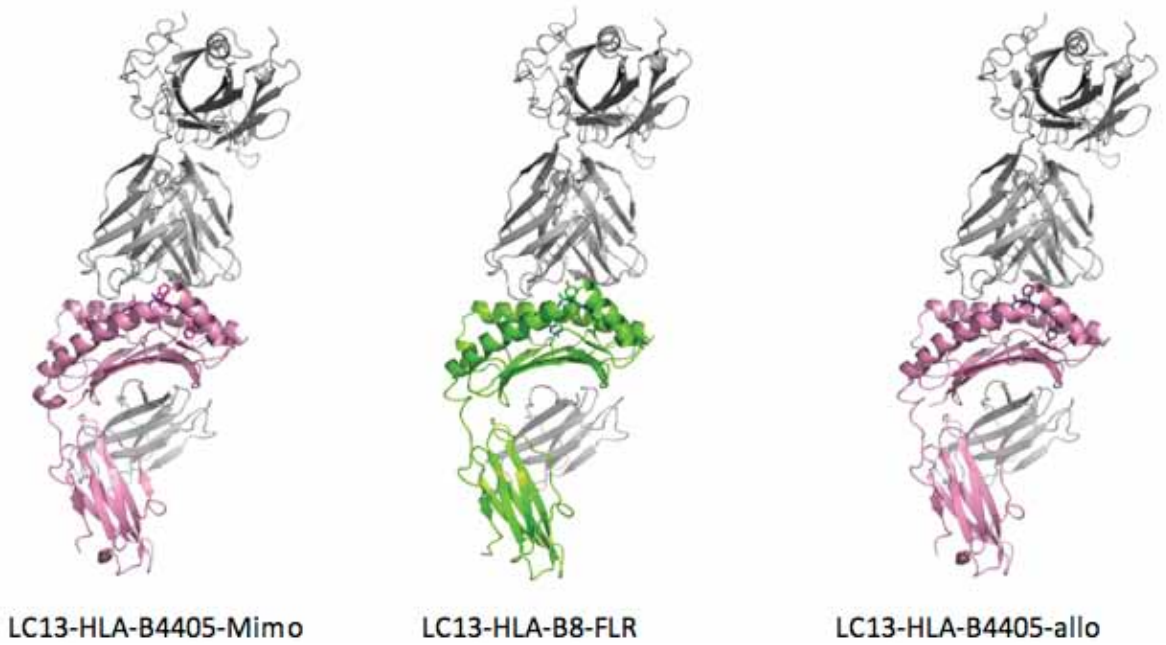

New information about the mechanisms that underlie T-cell alloreactions could help to reduce morbidity and mortality associated with tissue transplantation. Image: Jamie Rossjohn, Monash University

Towards better and earlier diagnosis of malaria

Discriminating the intraerythrocytic lifecycle stages of the malaria parasite using synchrotron FT-IR microspectroscopy and an artificial neural network

G.T. Webster, K.A. de Villiers, T.J. Egan, S. Deed, L. Tilley, M.J. Tobin, K.R. Bambery, D. McNaughton and B.R. Wood, Discriminating the Intraerythrocytic Lifecycle Stages of the Malaria Parasite Using Synchrotron FT-IR Microspectroscopy and an Artificial Neural Network, Anal. Chem., 81, 2516-2524, (2009). Impact factor 5.214.

Synchrotron Fourier transform infrared studies have paved the way for development of an automated infrared-based technology capable of diagnosing malaria at all stages of the parasite's lifecycle inside red blood cells.

One of the world's deadliest infectious diseases, malaria is caused by unicellular parasites of the genus *Plasmodium*. It afflicts over 500 million people and kills more than one million a year, almost all due to *P. falciparum*. The infection begins with the bite of a female *Anopheles* mosquito carrying *P. falciparum.*

The parasite spends part of its lifecycle inside red blood cells. These intraerythrocytic stages are the early 'ring' stage, the trophozoite phase, and finally the schizont stage, which is when the parasite replicates.

In its trophozoite phase, the parasite digests large quantities of haemoglobin and releases toxic free ferrous protoporphyrin IX (Fe(II)PPIX) and denatured globin. The Fe(II)PPIX is oxidised to Fe(III)PPIX and aggregates into an insoluble biomineral known as haemozoin (malaria pigment).

Bright-field microscopy has been the standard for malaria diagnosis since the disease was discovered in 1880. However, while microscopy can quantify and identify the different lifecycle stages, it requires experienced personnel. Rapid diagnostic tests (RDTs) or "dipsticks" that detect malarial antigen in blood samples are simple to use and allow on-the-spot diagnoses, but are expensive and cannot provide quantitative results. Laser desorption mass spectrometry can detect haemozoin but cannot identify the early ring stages. Raman microscopy also relies on detection of haemozoin.

The importance of lipids as catalysts for haemozoin formation is well documented. This means that a spectroscopic method for detecting lipid signatures in infected erythrocytes could be useful for distinguishing the early intraerythrocytic stages.

Although resonance Raman spectroscopy has been used to detect and monitor haemozoin formation in erythrocytes, the diagnostic potential of FT-IR spectroscopy has not hitherto been investigated. FT-IR is more sensitive to the lipid moieties than Raman spectroscopy, potentially enabling detection of parasites prior to haemozoin formation, and much faster. Red blood cells make ideal subjects for FT-IR synchrotron spectroscopy, since each erythrocyte is closely matched in size to the diameter of the synchrotron infrared beam (8 microns).

An international research collaboration has used the Australian Synchrotron to produce the first synchrotron Fourier transform infrared (FT-IR) spectra of fixed single erythrocytes (red blood cells or RBCs) infected with *Plasmodium falciparum* at different stages of the intraerythrocytic cycle.

The work demonstrates that synchrotron FT-IR spectroscopy in combination with multivariate statistical methods can detect the presence of haemozoin in single infected RBCs. The technique can also differentiate between the three parasitic lifecycle stages based on fatty acid composition within the infected erythrocytes. As well as the morphological differences observed between the parasite's intraerythrocytic lifecycle stages, there are specific changes in lipid composition that give rise to a very specific lipid signature in the 3100-2800 cm^{-1} region of the mid-IR spectrum.

Features attributable to haemozoin are not immediately obvious in the raw spectra of trophozoite-infected cells; so the researchers calculated a second-derivative difference spectrum between the control and the trophozoite spectrum.

To demonstrate the diagnostic utility of FT-IR spectroscopy, the researchers employed an artificial neural network (ANN) to unambiguously differentiate the different stages of the parasite. The results pave the way for an automated infrared-based technology capable of diagnosing malaria at all intraerythrocytic stages.

Finding inexpensive, sensitive and rapid methods for malaria diagnosis that require minimal training for technicians would have a major impact on malaria management. FT-IR spectroscopy may offer several advantages, including ability to detect all lifecycle stages including the early ring stage prior to haemozoin formation, and unambiguous non-subjective diagnosis based on neural network spectral pattern recognition. Although the instrumentation is currently expensive, actual cost per test is very low, especially with inexpensive substrates such as commercially available infrared reflecting microscope slides. The technique's sensitivity is 1 parasite/μL of blood on a thin film when using a synchrotron source.

While a synchrotron source is not suited for a clinical environment, ongoing instrumentation and software development could potentially lead to FT-IR spectroscopy becoming a new weapon in the fight against malaria.

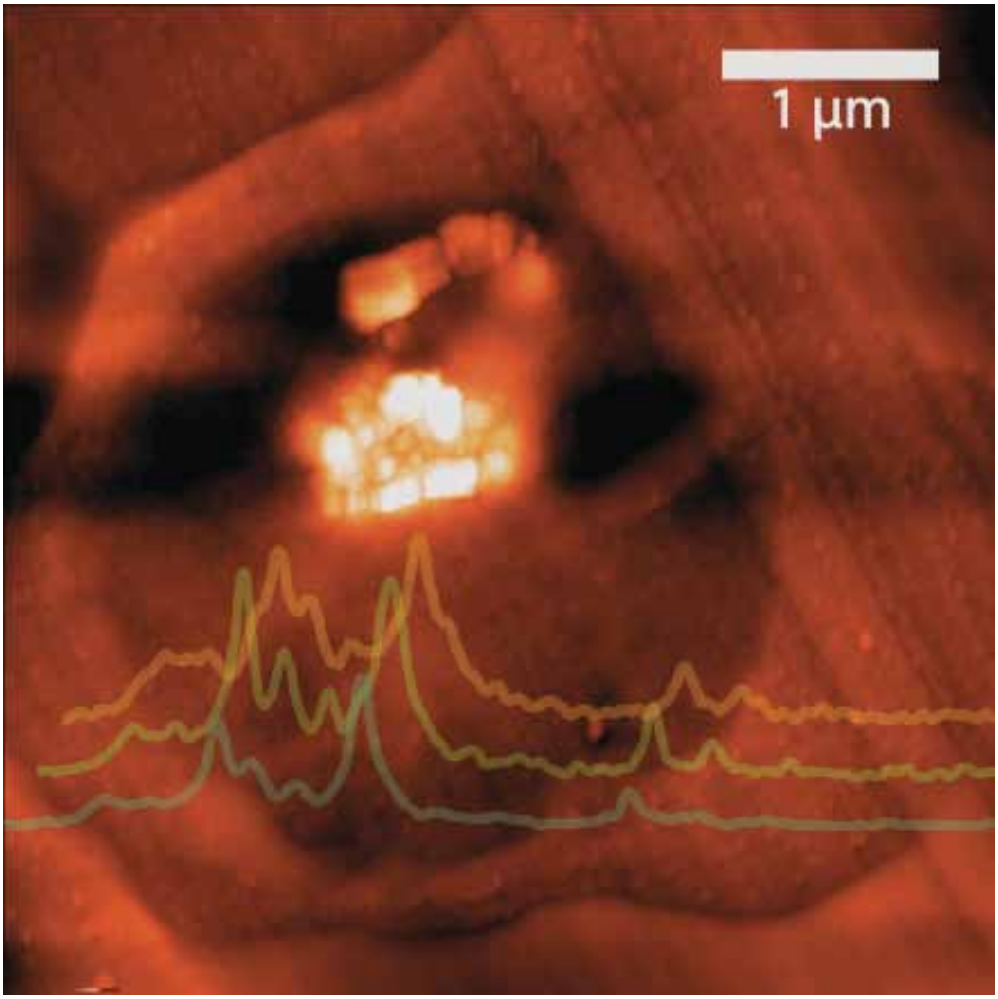

Atomic force microscopic image of haemozoin (malaria pigment), an important biomarker used for the identification of the malaria parasite inside a single red blood cell using synchrotron infrared spectroscopy. Image supplied by Volker Deckert, University of Jenna. Reprinted with permission from G.T. Webster, K.A. de Villiers, T.J. Egan, S. Deed, L. Tilley, M.J. Tobin, K.R. Bambery, D. McNaughton and B.R. Wood, Discriminating the Intraerythrocytic Lifecycle Stages of the Malaria Parasite Using Synchrotron FT-IR Microspectroscopy and an Artificial Neural Network, Anal. Chem., 81, 2516-2524, (2009). Copyright 2011 American Chemical Society.

Nitrogen doping of ZnO semiconductor films

Study of a nitrogen-doped ZnO film with synchrotron radiation

C.W. Zou, X.D. Yan, J. Han, R.Q. Chen, W. Gao and J. Metson, Study of a nitrogen-doped ZnO film with synchrotron radiation, Applied Physics Letters 94, 171903-1 to 171903-3 (2009). Impact factor 3.554.

Close examination of the structure and chemical states of nitrogen atoms in nitrogen-doped zinc oxide films suggests that specific annealing temperatures are required for creation of *p*-type semiconductor zinc oxide films, which could potentially be used in many optoelectronic applications.

Semiconductors such as silicon have many uses in electronic and optoelectronic devices – including transistors, telephones, integrated circuits, diodes, lasers and photovoltaic cells – because their electrical conductivity can be manipulated in a controllable way by doping them with small quantities of other elements. Binary semiconductors consist of two elements; their advantages over single-element semiconductors include faster operation, greater robustness at high temperature and a broader range of optoelectronic characteristics.

P-type semiconductors have dopant atoms that can accept electrons from the bulk material, creating an excess of 'holes' into which electrons can move. *N*-type semiconductors have dopant atoms that can donate electrons to the bulk material, creating an excess of free electrons. Both types are needed for most semiconductor applications.

The binary semiconductor zinc oxide has attracted considerable attention worldwide for its potential devices applications. However, fabrication of *p*-type ZnO is is still a challenge because of the self-compensation effect from native defects such as zinc and other atoms that are out of place in the lattice (interstitial atoms). For example, oxygen vacancies and zinc interstitials can donate extra electrons that may detract from the process of 'hole' formation.

Nitrogen is generally regarded as the most promising candidate for *p*-type doping of ZnO films because its radius is similar to oxygen. However, although the low solubility of nitrogen acceptors in ZnO can be overcome, doping efficiency and stability are still not good enough and the nitrogen doping mechanism is not clear.

Chongwen Zou and Wei Gao from the University of Auckland in New Zealand used x-ray absorption near-edge spectroscopy (XANES) and photoelectron spectroscopy (PES) on the soft x-ray beamline at the Australian Synchrotron to systematically investigate the mechanism of nitrogen doping and the effects of annealing temperature on the doping process.

XANES is a powerful tool for investigating the local environment around atoms, providing element-specific information about chemistry, site occupancy and the neighbouring environment. However, other researchers have reported conflicting results from XANES studies of nitrogen-doped ZnO, such as whether low or high annealing temperatures are more effective.

Zou and Gao prepared their *p*-type ZnO:N films by thermal oxidation of Zn_3N_2 samples. The films were cleaned by argon ion (Ar^+) bombardment until no carbon-related signals could be detected by x-ray photoelectron spectroscopy (XPS). The synchrotron XPS results were far clearer than those obtained by laboratory XPS, enabling the researchers to study the complex nitrogen 1s spectra in samples annealed at 450, 550 and 600°C. With higher annealing temperatures, the peak associated with nitrogen molecules $(N_2)_o$ at oxygen sites decreased markedly and a new peak appeared, most likely associated with nitrogen atoms $(N)_o$ at oxygen sites. These nitrogen atoms are regarded as the acceptors, and responsible for the *p*-type characteristics of nitrogen-doped ZnO films.

XANES measurements around the nitrogen *K*-edge produced spectra with seven main peaks associated with 1*s* to 2*p* π^* and other electronic transitions in the N-Zn bond. The spectra indicate a greatly reduced nitrogen molecule contribution for an annealing temperature of 550°C, consistent with the PES results. Experimental results for the 550 and 600°C samples agree with the theoretical simulation, indicating that the residual nitrogen atoms occupy the oxygen sites and become $(N)_o$ acceptors at these annealing temperatures.

Overall, the results indicate that ZnO:N films show *p*-type behaviour after annealing at 500 and 550°C, and come back to *n*-type behaviour after annealing at 600°C. The researchers proposed a mechanism to explain this behaviour. They concluded that the nitrogen atoms that behave as acceptors are metastable and sensitive to annealing temperature, and that *p*-type doping of ZnO with nitrogen dopants can only be realised after annealing within a suitable temperature window.

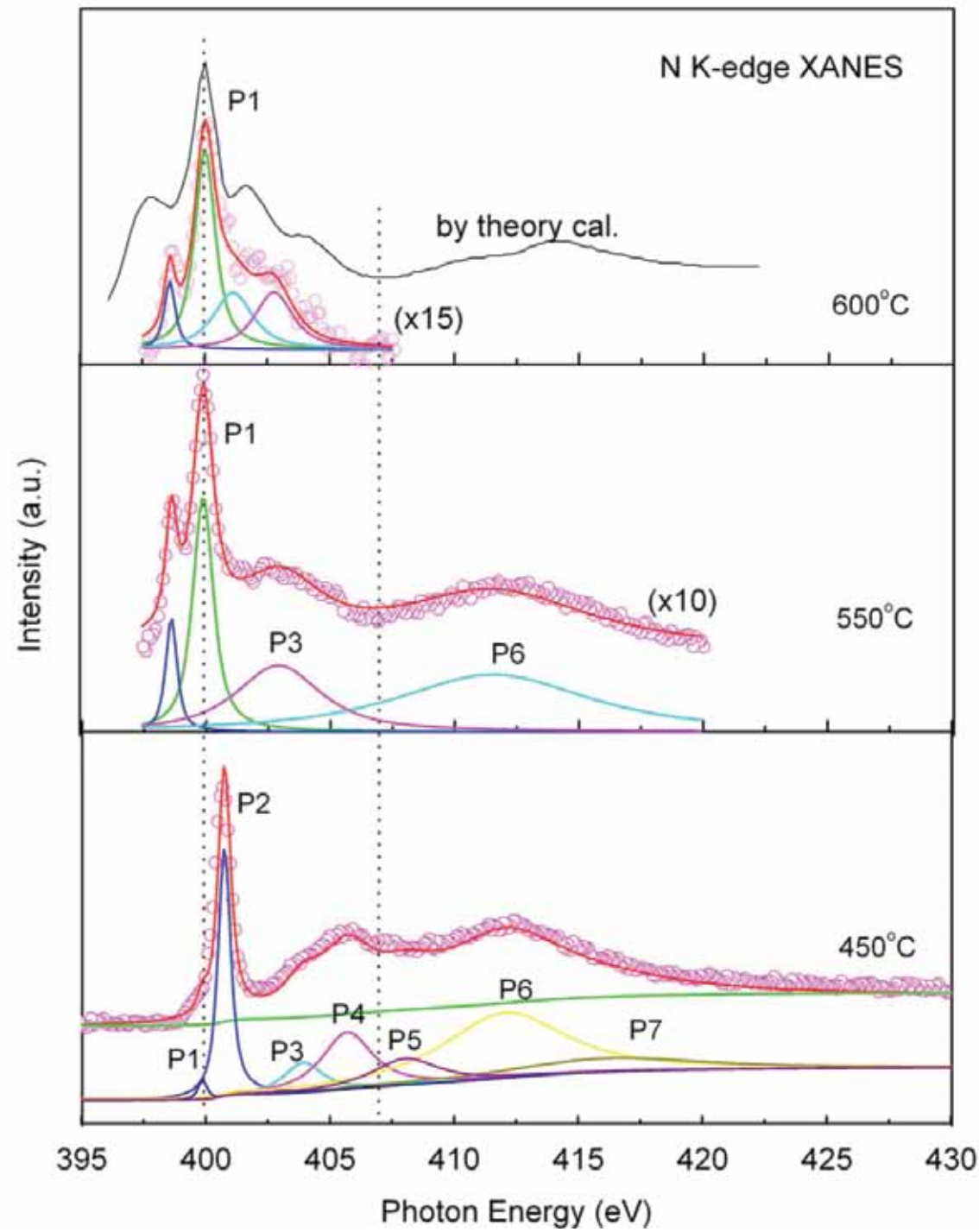

Peaks due to electron transitions in nitrogen K-edge NEXAFS spectra show that annealing nitrogen-doped ZnO films at higher temperatures leads to the residual nitrogen atoms occupying the O sites and becoming (N)o acceptors. Image: Chongwen Zou, Auckland University. Reprinted with permission from Figure 3 from: C.W. Zou, X.D. Yan, J. Han, R.Q. Chen, W. Gao and J. Metson, Study of a nitrogen-doped ZnO film with synchrotron radiation, Applied Physics Letters 94, 171903-1 to 171903-3 (2009). Copyright 2009, American Institute of Physics.

High-definition trace element imaging

The new Maia detector system: methods for high definition trace element imaging of natural material

C.G. Ryan, D.P. Siddons, R. Kirkham, P.A. Dunn, A. Kuczewski, G. Moorhead, G. De Geronimo, D.J. Paterson, M.D. de Jonge, R.M. Hough, M.J. Lintern, D.L. Howard, P. Kappen and J. Cleverley, The New Maia Detector System: Methods For High Definition Trace Element Imaging Of Natural Material, International Conference on x-ray Optics and Microanalysis, Karlsruhe, September 2009, AIP Conference Series, 1221, 9-17 (2010).

The Maia detector array has demonstrated megapixel high-definition trace element imaging on the x-ray fluorescence microscopy (XFM) beamline at the Australian Synchrotron, with faster acquisition and improved counting statistics.

Microscopy and microanalysis are critical tools for research in the geological and environmental sciences. Clues to process and evolution occur on spatial scales ranging from nanoparticles and micron-scale minerals to textural features such as zonation and alteration through subtle variation at the hand-specimen scale and on up to the scale of macroscopic geological features.

With the new XFM beamline at the Australian Synchrotron providing intense focused hard x-ray beams, the challenge is to efficiently capture spatial detail over four orders of magnitude from the micron scale to the scale of a few centimetres in images approaching 100M pixels.

Motivated by the goal of megapixel trace element imaging and the challenge of increasing collection solid-angle and count-rate capacity to gain adequate statistics in so many pixels, researchers from CSIRO and Brookhaven National Laboratory have developed a large energy-dispersive detector array called Maia for synchrotron x-ray fluorescence (SXRF) elemental imaging on the XFM beamline and on beamlines at the National Synchrotron Light Source.

The complexity of SXRF spectra in geoscience and environmental applications demands a full spectral approach to imaging to unfold overlapping contributions from interfering elements and detector artefacts. Complex SXRF data can be decomposed into elemental components using a matrix transform method called Dynamic Analysis (DA), originally developed for PIXE (proton-induced x-ray emission) imaging. The Maia concept is to use a large detector array and real-time processing techniques to apply the DA method to each event in turn to project images in real-time.

The researchers initially used their DA imaging method on data from the Advanced Photon Source to probe the spatial distribution and speciation of specific pathfinder elements (e.g. Au, Cu, As) in regolith material from the Moolart Wells gold deposit in Western Australia. In this material, the presence of gold is masked by some particularly challenging peak overlaps. The DA method successfully separated gold from the overlaps to produce a unique image for gold that contrasts other elemental distributions and appears free of discernable artefacts.

The XFM beamline was then used to examine a heavy mineral (rutile) concentrate sample from an Australian mineral sands deposit and a calcrete thin-section sample from the Mount Gibson gold deposit in WA. The Maia detector and integrated real-time processing system enabled images up to 77 megapixels to be acquired that capture spatial detail over 3-4 orders of magnitude with collection times of 3-10 hours. Preliminary images were acquired at 500 x 500 pixel definition in 10 minutes.

Applying Maia to geological samples provided images with fine textural detail captured within a broader spatial and chemical context. A feature of SXRF imaging is its sensitivity and, due to the large depth of focus of the lens system and penetration of fluoresced x-rays, its ability to detect rare small particles at depth within a sample section. In the Mount Gibson example, rare sub-micron gold particles were detected in correlation with the infiltrating veins, suggesting that gold is carried by the fluids, or remobilised from calcrete, and is precipitated in the veins in contact with the unaltered calcrete.

Update: the Maia detector

The Maia detector reported here comprises 96 elements in an 8x12 rectangular array. A new Maia with 384 detector elements in an annular array has recently begun user experiments at the XFM beamline. The system's processor can perform deconvolution at up to 50M events per second and has easily handled the upgrade, which now provides a further six-fold increase in solid angle and counting rates.

In June 2011, the Maia detector won a prestigious R&D 100 award from R&D Magazine, an award that recognises the 100 most significant technological products to enter the world market.

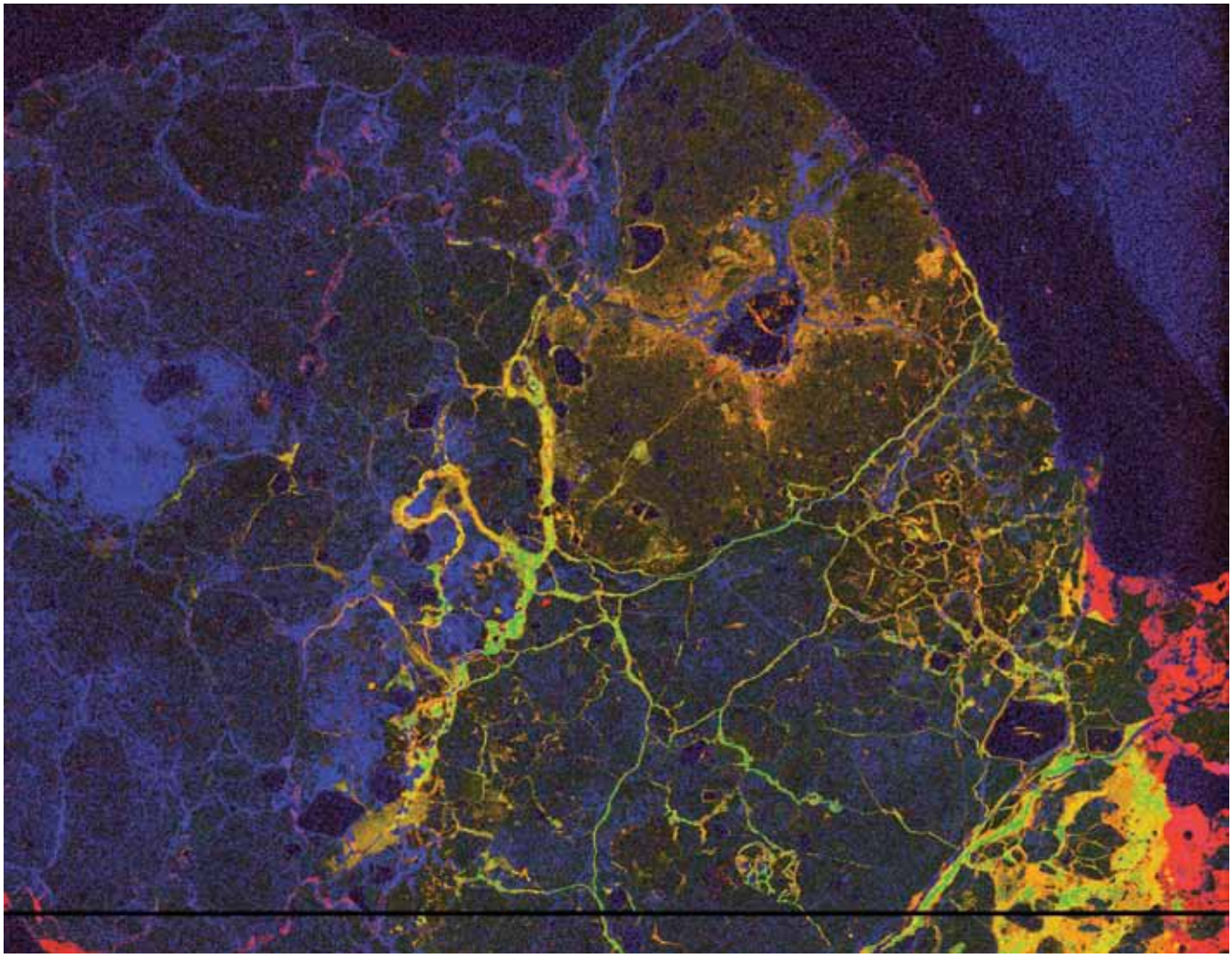

X-ray fluorescence microscopy image (9600 x 8000 pixels) of a thin section of calcrete from the Mount Gibson gold deposit in Western Australia showing the elements As (red), Fe (green) and Br (blue), acquired using the new Maia detector at the Australian Synchrotron. Image courtesy of Chris Ryan and Mel Lintern (CSIRO). Ryan et al., AIP Conf. Series 1211 (2010) 9-17.

$Sr_xCa_{1-x-y}Nd_yMnO_3$ perovskites and the Jahn-Teller effect

Structural characterisation of the perovskite series $Sr_xCa_{1-x-y}Nd_yMnO_3$: Influence of the Jahn–Teller effect

B.J. Kennedy, P.J. Saines, J. Ting, Q. Zhou and J.A. Kimpton, Structural characterisation of the perovskite series $Sr_xCa_{1-x-y}Nd_yMnO_3$: Influence of the Jahn–Teller effect, Journal of Solid State Chemistry 182 (2009) 2858–2866 . Impact factor 2.34

Powder diffraction is an invaluable tool for conducting parametric studies of perovskite structures, providing an overview of form and function that is important for harnessing the useful electronic and magnetic properties of these versatile materials. Researchers recently investigated a series of doped perovskite manganites with varying ratios of strontium, calcium and neodymium.

As a result of their enormous structural and compositional flexibility, which give rise to interesting and useful physical properties, perovskite-type materials have numerous commercial applications such as medical sensors, microphone and mobile phone components, hydrogen fuel cells and sonar transducers. Perovskite-type oxides can be fine-tuned to take advantage of particular electronic or magnetic functional capabilities (such as the type of magnetism or the ability to conduct or not conduct electrons) that arise as a result of the atomic structure of the material; this sensitivity of function to structure may also be exploited through application of external stimuli such as temperature or pressure.

As part of a broad study of perovskite-type oxides, researchers from the University of Sydney used powder diffraction at the Australian Synchrotron to determine the precise structures and phase transitions observed in response to temperature changes between room temperature and 500°C in two series of $Sr_xCa_{1-x-y}Nd_yMnO_3$ perovskite manganites, where y=0.1 or y=0.2, and x=0.1, 0.2, 0.3,...1.0.

In 1937, Jahn and Teller proposed a theorem that predicts the structural distortion of non-linear molecules with degenerate energy states. The distortion that they undergo has the effect of lowering the overall energy state of the molecule and is commonly observed in highly symmetrical molecules, such as octahedrally coordinated transition metals with appropriate distribution of d-electrons. This is thus called the Jahn-Teller (JT) effect.

Over the years, the Jahn–Teller (JT) effect has attracted considerable interest from chemists and physicists, initially to gain a fundamental understanding of the properties of molecules and crystals, but increasingly to explain technologically important, but complex, phenomena such as superconductivity in cuprates and magnetoresistance in manganites.

More recently, the complex interplay between the structure and the magnetic and electronic properties in perovskite manganites has motivated numerous studies of mixed valence oxides of the general type $A_{1-x}R_xMnO_3$ where A is an alkaline earth cation and R a lanthanide cation. There are many examples of unusual properties of these oxides that are strongly influenced by distortions associated with the presence of the JT-active Mn^{3+} cation. An example is that a modest amount of doping in the $La_{1-x}Sr_xMnO_3$ system transforms the canted anti-ferromagnet into a ferromagnetic insulator and with further doping into a ferromagnetic metal.

The authors have previously reported temperature-induced phase transitions of $SrMnO_3$ doped with cerium and observed both long-range ordering of the JT tilted MnO_6 octahedra and cooperative tilting of the MnO_6 octahedra. However, using Ce gives rise to the possibility of mixed valency, i.e. Ce^{3+} and Ce^{4+}. In the current study the use of neodymium (Nd^{3+}) instead of cerium removes the potential impact of cation valency on the structural transitions and on the ability to identify the extent of Jahn-Teller-active Mn^{3+} cations.

Orbital ordering rarely occurs in orthorhombic *Pbnm* manganese perovskites, with $LaMnO_3$ being an important exception. Strontium-rich samples in the $Sr_{0.9-x}Ca_xCe_{0.1}MnO_3$, however, have a tetragonal structure with the MnO_6 octahedra exhibiting a noticeable elongation due to orbital ordering. Heating selected members of this series results in a transition to the cubic perovskite structure in which the orbital ordering and octahedral tilting disappear in two distinct stages.

In this paper, the authors report that the room-temperature structures of the $Sr_xCa_{0.9-x}Nd_{0.1}MnO_3$ perovskite series, x=0.9, 0.8, 0.7,...0.0, vary in symmetry across the series from cubic $Pm\bar{3}m$ ⟷ tetragonal *I4/mcm* ⟷ orthorhombic *Pbnm* and in the series $Sr_xCa_{0.8-x}Nd_{0.2}MnO_3$ where x=0.8, 0.7, 0.6...0.0 the symmetry varies tetragonal *I4/mcm* ⟷ orthorhombic *Pbnm*.

Orbital ordering is apparent in the tetragonal oxides, as revealed by the tetragonal elongation of the MnO_6 octahedra. High-temperature diffraction measurements identify an apparently continuous, isosymmetric (*I4/mcm* to *I4/mcm*) phase transition associated with the loss of long-range orbital ordering (and the cooperative JT distortion), and continuous evolution of the

octahedral tilt angle. Heating the manganites to still higher temperatures results in a continuous transition to the cubic *Pm3̄m* structure. The orthorhombic structures (*Pbnm*) do not exhibit orbital ordering and although a first order transition to the tetragonal structure is observed in $Sr_{0.4}Ca_{0.5}Nd_{0.1}MnO_3$, this high-temperature tetragonal structure does not exhibit orbital ordering.

Perovskite structures such as those reported in this paper are versatile materials with useful electronic and magnetic properties. Powder diffraction is an invaluable tool for conducting parametric studies that provide an overview of the materials' form and function; in this case being used specifically to examine crystal structure and phase transitions arising from variation of sample temperature.

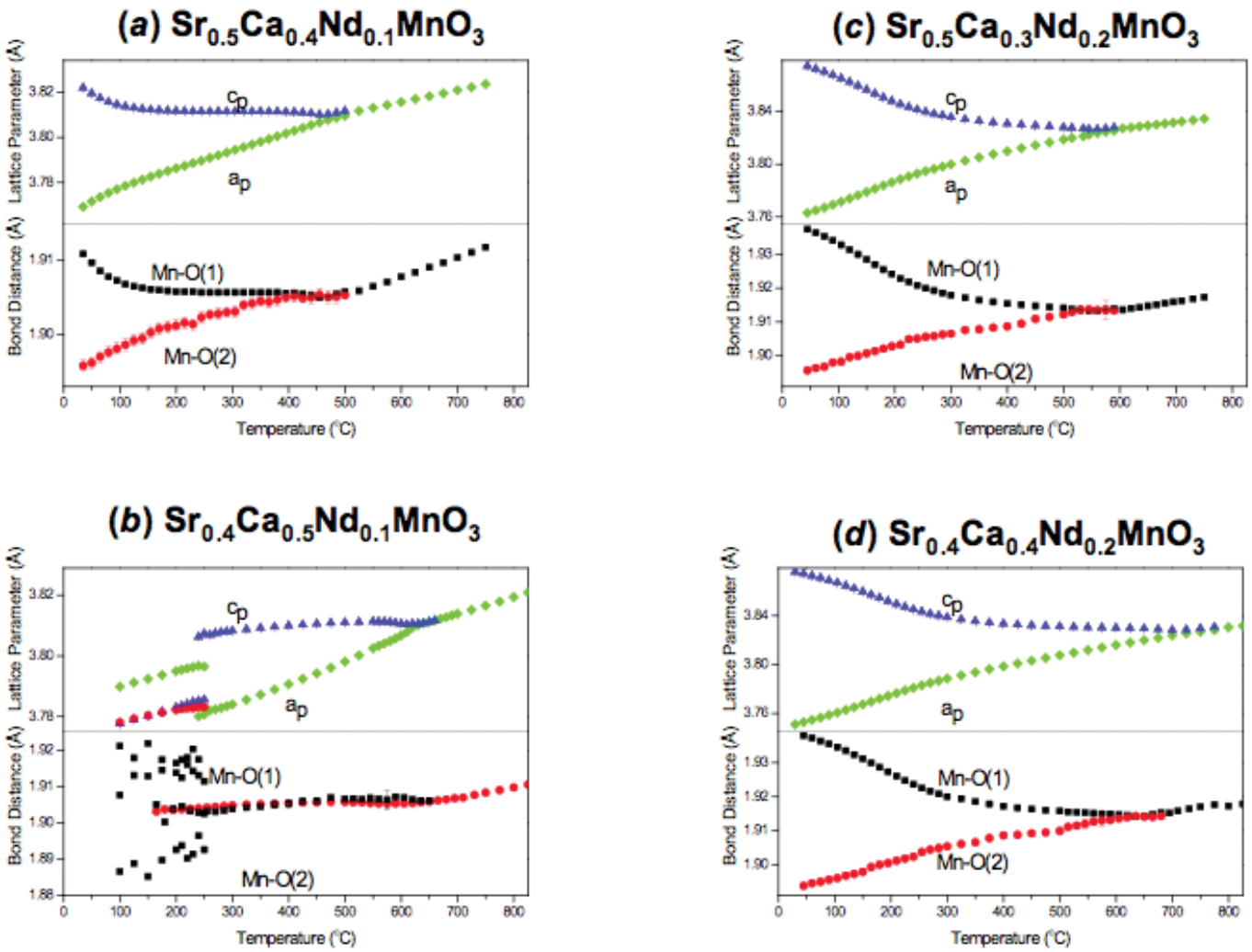

Variation of scaled lattice parameters and Mn-O bond distances in selected members of the $Sr_xCa_{1-x-y}Nd_yMnO_3$ series (y = 0.1, x = 0.4 or 0.5 and y = 0.2, x = 0.4 or 0.5) with temperature, as shown by high-temperature synchrotron x-ray diffraction studies. Transitions in (a), (c) and (d) are tetragonal to cubic. Transitions in (b) are from orthorhombic to mixed Pnma and I4/mcm to pure tetragonal to pure cubic.

Feed forward-feedback system for electron beam stability

Development of a combined feed forward-feedback system for an electron Linac

E. Meier, S.G. Biedron, G. LeBlanc, M.J. Morgan, J. Wue, Development of a combined feed forward-feedback system for an electron Linac, Nucl. Instrum. Meth. A, 609, 79-88, (2009). Impact factor 1.317.

A promising new approach to stabilising electron beams combines feedback control with neural network feed-forward techniques. Developed at the Australian Synchrotron as part of an international project, the new system will help ensure the best possible light quality at next-generation light sources.

The next generation of synchrotron light sources being developed around the world will use free-electron laser (FEL) sources to produce synchrotron light of even greater brilliance than current (third-generation) sources like the Australian Synchrotron. Producing light of this quality requires high stability in the longitudinal parameters (energy and energy spread) of the electron beam.

This paper describes the development of a neural network or advanced control algorithm designed to stabilise the energy of an electron beam from a linear accelerator (linac).

The ultimate aim of the work is a precise and robust control system that will stabilise electron beam energy and energy spread for the FERMI@Elettra free electron laser being constructed at the Elettra synchrotron in Italy.

The approach described in this paper combines a conventional proportional-integral (PI) controller with a neural network (NNET) feed-forward algorithm. Combining the robustness of PI control with the capabilities of a feed-forward system enables control over a wider range of frequencies. The team chose neural networks to operate the feed-forward task because of their proven ability to learn and adapt. This is believed to be the first time that neural networks have been used to control longitudinal beam parameters in a feed-forward way.

Artificial neural networks are based on mathematical models of biological neural networks. They are adaptive systems that can change structure based on sets of inputs and outputs presented during the learning phase. Each network consists of an input layer and an output layer of neurons, with a 'hidden' layer (sometimes more than one) in-between.

The AS linac (see diagram on opposite page) consists of an electron gun, focussing elements (solenoids and quadrupoles), and bunching and accelerating sections supplied by klystrons (radiofrequency amplifiers). Bunch characteristics are controlled by a 500 MHz sub-harmonic pre-buncher (SPB), a 3 GHz primary buncher (PBU) and a 3 GHz final buncher (FBU).

Perturbations in longitudinal parameters such as energy mostly come from jitter (variations) in the klystron output. For these experiments, jitter was induced in the phase and voltage of klystron 1, which affects the PBU, FBU and first accelerating section (ACC1). The second accelerating section (ACC2), which is only supplied by klystron2, acted as the control.

The team trained their NNET to recognise jitter in phase and voltage for one of the linac's two klystrons, and to predict future energy deviations. The neural network was only provided with information on klystron phase and voltage and its response was not affected by perturbations in other elements in the line. In a two-stage control process, past values of klystron phase and voltage were fed into the neural network, which predicts the next klystron pulse deviation. The second stage used the NNET prediction to compute the feed-forward correction and combines it with the PI control algorithm. For stability reasons, the NNET response is bounded to the maximum response determined during the training phase.

The researchers collected three sets of data. The first set was used to evaluate appropriate neural network topologies for a single frequency. The second was used to train the network for the single frequency case. The third was used to evaluate the topology and train two neural network types – a hyperbolic tangent network (HTN) and a radial basis function (RBF) network – for a multi-frequency study.

Tests confirmed that the HTN topology chosen for the single frequency study was viable for any combination of voltage and frequency in the data set. Evaluation of the HTN showed similar performance to that obtained on the training data, indicating the network's capability to successfully deal with amplitudes and frequencies different from the training data but within the same range.

Although RBF network design requires less data and can be much faster than HTNs, RBF performance seems slightly poorer. The results demonstrate the network's ability to interpolate its predictions when the encountered frequency is within the training range.

In summary, these experiments in an operating accelerator environment demonstrated the controller's capability to cancel single and multi-frequency jitter, as well as the successful augmentation of the NNET by the PI algorithm. The preliminary results obtained on the Australian Synchrotron Linac were encouraging, and this strategy will be pursued for complementing a feed forward-feedback system based on neural networks for the new FERMI@Elettra FEL.

More sophisticated experiments on the LCLS machine have been used to investigate neural network performance for higher frequency jitter and higher repetition rates.

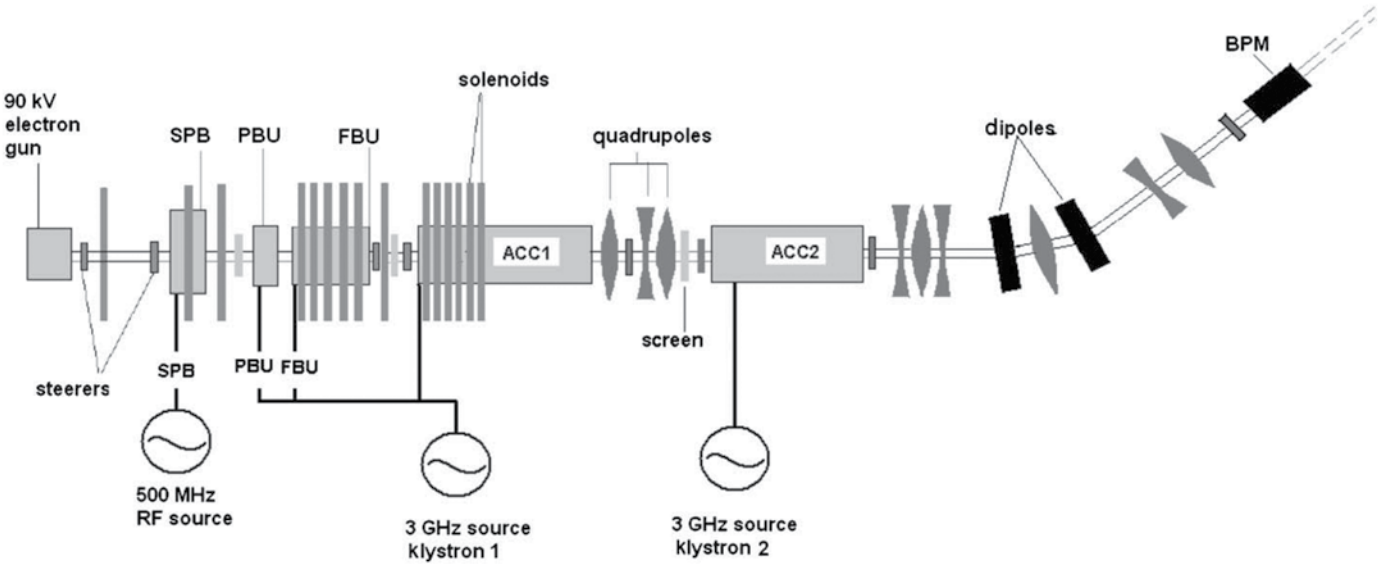

In the Australian Synchrotron Linac assembly, a sub-harmonic pre-buncher (SPB), primary buncher (PBU) and final buncher (FBU) bunch the electron stream from the gun. Two accelerating sections (ACC1 and ACC2) bring the beam to 100 MeV. A beam position monitor (BPM) located after the bending magnets detects energy variations. Reproduced by permission of Nuclear Instruments and Methods in Physics Research Section A.

Publications and Presentations 2007 - 2009

Publications and Presentations 2007 - 2009

W.H. Ang, L.J. Parker, A. De Luca, L. Juillerat-Jeanneret, C.J. Morton, M. Lo Bello, M.W. Parker and P.J. Dyson, Rational Design of an Organometallic Glutathione Transferase Inhibitor. *Angew. Chem. Int. Edit.,* 48, 3854-3857, (2009).

L.L. Araujo, R. Giulian, P. Kluth, B. Johannessen, D.J. Cookson, G.J. Foran, M.C. Ridgway, Properties of Ge nanocrystals determined by EXAFS and SAXS, *Adv. Sync. Rad.,* 1, 169-178, (2008).

L.L. Araujo, G.J. Foran and M.C. Ridgway, Multiple scattering effects on the EXAFS of Ge nanocrystals, *J. Phys. - Condens. Mat.,* 20, 165210, (2008).

L.L. Araujo, R. Giulian, D.J. Sprouster, C.S. Schnohr, D.J. Llewellyn, and P. Kluth, D.J. Cookson, G.J. Foran, M.C. Ridgway, Size-dependent characterization of embedded Ge nanocrystals: Structural and thermal properties, *Phys. Rev. B,* 78, 094112, (2008).

S.C. Atkinson, R.C.J. Dobson, J.M. Newman, M.A. Gorman, C. Dogovski, M.W. Parker and M.A. Perugini, Crystallization and preliminary x-ray analysis of dihydrodipicolinate synthase from Clostridium botulinum in the presence of its substrate pyruvate, *Acta Crystallogr. F,* 65, 253-255, (2009).

M. Backman, F. Djurabekova, O. H. Pakarinen, K. Nordlund, L. L. Araujo and M. C. Ridgway, Amorphization of Ge and Si nanocrystals embedded in amorphous SiO2 by ion irradiation, *Phys. Rev. B,* 80, 144109, (2009).

A.J. Berry, A.M. Walker, J. Hermann, H.St.C. O'Neill, G.J. Foran, J.D. Gale, Titanium substitution mechanisms in forsterite, *Chem. Geol.,* 242, 176-186, (2007).

A.J. Berry, L.V. Danyushevsky, H. St C. O'Neill, M. Newville and S.R. Sutton, Oxidation state of iron in komatiitic melt inclusions indicates hot Archaean mantle, *Nature,* 455, 960-964, (2008).

S.K. Bhargava, D.B. Akolekar, G. Foran, Investigations on gold nanoparticles supported on rare earth oxide catalytic materials, *J. Mol. Catal. A - Chem.,* 267, 57-64, (2007).

V.K. Bhatia, C.S. Kealley, R. Wuhrer, K.S. Wallwork and M.B. Cortie, Ternary beta and gamma phases in the Al-Au-Cu system at 750 degC, *J. Alloy. Compd.,* 488, 100-107, (2009).

J.M. Booth and P.S. Casey, Anisotropic Structure Deformation in the VO2 Metal-Insulator Transition, *Phys. Rev. Lett.,* 103, 086402, (2009).

S.J. Borg, J.W. Tye, M.B. Hall and S.P. Best, Assignment of Molecular Structures to the Electrochemical Reduction Products of Diiron Compounds Related to [Fe-Fe] Hydrogenase: A Combined Experimental and Density Functional Theory Study, *Inorg. Chem.,* 46, 384-394, (2007).

J.D. Bourke, C.T. Chantler, C. Witte, Finite difference method calculations of x-ray absorption fine structure for copper, *Phys. Lett. A,* 360, 702-706, (2007).

E. Bovell, C.E. Buckley, W. Chua-anusorn, D. Cookson, N. Kirby, M. Saunders and T.G. St Pierre, Dietary iron-loaded rat liver haemosiderin and ferritin: in situ measurement of iron core nanoparticle size and cluster structure using anomalous small-angle x-ray scattering, *Phys. Med. Biol.,* 54, 1209-1221, (2009).

J. Brugger, B. Etschmann, W. Liu, D. Testemale, J.L. Hazemann, H. Emerich, W. van Beek, O. Proux, An XAS study of the structure and thermodynamics of Cu(I) chloride complexes in brines up to high temperature (400 degC, 600 bar), *Geochim. Cosmochim. Ac.,* 71, 4920-4941, (2007).

A.N. Buckley, S.W. Goh, W.M. Skinner, R. Woods, L-J. Fan, Interaction of cuprite with dialkyl dithiophosphates, Int. *J. Min. Process.,* 93, 155-164, (2009).

B.R. Burgess, R.C.J. Dobson, M.F. Bailey, S.C. Atkinson, M.D.W. Griffin, G.B. Jameson, M.W. Parker, J.A. Gerrard and M.A. Perugini, Structure and Evolution of a Novel Dimeric Enzyme from a Clinically Important Bacterial Pathogen, *J. Biol. Chem.,* 283, 27598-27603, (2008).

B.R. Burgess, R.C.J. Dobson, C. Dogovski, G.B. Jameson, M.W. Parker and M.A. Perugini, The purification, crystallisation and preliminary x-ray diffraction studies to near atomic resolution of dihydrodipicolinate synthase from methicillin-resistant Staphylococcus aureus, *Acta Crystallogr. F,* 6, 659-661, (2008).

E.D. Burton, R.T. Bush, L.A. Sullivan, S.G. Johnston, R.K. Hocking, Mobility of arsenic and selected metals during re-flooding of iron- and organic-rich acid-sulfate soil, *Chem. Geol.,* 253, 64-73, (2008).

E.D. Burton, R.T. Bush, S.G. Johnston, K.M. Watling, R.K. Hocking, L.A. Sullivan and G.K. Parker, Sorption of Arsenic(V) and Arsenic(III) to Schwertmannite, *Environ. Sci. Technol.,* 43, 9202-9207, (2009).

N.S. Butler, A. Theodossis, A.I. Webb, M.A. Dunstone, R. Nastovska, S.H. Ramarathinam, J. Rossjohn, A.W. Purcell and S. Perlman, Structural and Biological Basis of CTL Escape in Coronavirus-Infected Mice, *J. Immunol.,* 180, 3926-3937, (2008).

A.J. Canty, Organopalladium and platinum chemistry in oxidising milieu as models for organic synthesis involving the higher oxidation states of palladium, *Dalton T.,* 47, 10409-10417, (2009).

A.J. Canty, M.G. Gardiner, R.C. Jones, T. Rodemann and M. Sharma, Binuclear Intermediates in Oxidation Reactions: [(Me3SiC-triple bond-C)Me2(bipy)Pt-PtMe2(bipy)]+ in the Oxidation of Pt(II)Me2(bipy) (bipy) = 2,2'-Bipyridine) by IPh(C-triple bond-CSiMe3)(OTf) (OTf = Triflate), *J. Am. Chem. Soc.,* 131, 7236-7237, (2009).

A.P. Chandra, A.R. Gerson, A review of the fundamental studies of the copper activation mechanisms for selective flotation of the sulfide minerals, sphalerite and pyrite, *Adv. Colloid Interfac.,* 145, 97-110, (2009).

Publications and Presentations 2007 - 2009

C.T. Chantler, N.A. Rae, C.Q. Tran, Accurate determination and correction of the lattice parameter of LaB6 (standard reference material 660) relative to that of Si (640b), *J. App. Cryst.,* 40, 232-240, (2007).

C.T. Chantler, Development and applications of accurate measurement of x-ray absorption: The x-ray extended range technique for high accuracy absolute XAFS by transmission and fluorescence, *Eur. Phys. J. - Spec. Top.,* 169, 147-153, (2009).

M.H. Cheah, S.J. Borg and S.P. Best, Steps along the Path to Dihydrogen Activation at [FeFe] Hydrogenase Structural Models: Dependence of the Core Geometry on Electrocatalytic Proton Reduction, *Inorg. Chem.,* 46, 1741-1750, (2007).

J.-H. Chen, M.-Z. Zhang, Z.-T. Zhao, Orbit response matrix analysis and lattice periodicity restoration of the SSRF storage ring, *Chinese Phys. C,* 33, 785-788, (2009).

T. Chimdi, E.G. Robertson, L. Puskar, C.D. Thompson, M.J. Tobin, D. McNaughton, High resolution synchrotron FTIR spectroscopy of the far infrared v10 and v11 bands of R152a (CH3CHF2), *Chem. Phys. Lett.,* 465, 203-206, (2008).

T. Chimdi, E.G. Robertson, L. Puskar, C.D. Thompson, M.J. Tobin, D. McNaughton, Ro-vibrational analysis of the v9 and v16 bands of R152a, *J. Mol. Spectrosc.,* 251, 256-260, (2008).

N.P. Cowieson, G. King, D. Cookson, I. Ross, T. Huber, D.A. Hume, B. Kobe and J.L. Martin, Cortactin Adopts a Globular Conformation and Bundles Actin into Sheets, *J. Biol. Chem.,* 283, 16187-16193, (2008).

D.C. Creagh, M.E. Kubik, M. Sterns, On the feasibility of establishing the provenance of Australian Aboriginal artefacts using synchrotron radiation x-ray diffraction and proton-induced x-ray emission, *Nucl. Instrum. Meth. A,* 580, 721-724, (2007).

D. Creagh, A. Lee, V. Otieno-Alego, M. Kubik, Recent and future developments in the use of radiation for the study of objects of cultural heritage significance, *Radiat. Phys. Chem.,* 78, 367-374, (2009).

M.D. de Jonge, C.Q. Tran, C.T. Chantler, Z. Barnea, B.B. Dhal, D. Paterson, E.P. Kanter, S.H. Southworth, L. Young, M.A. Beno, J.A. Linton and G. Jennings, Measurement of the x-ray mass attenuation coefficient and determination of the imaginary component of the atomic form-factor of tin over the energy range of 29-60 keV, *Phys. Rev. A,* 75, 032702, (2007).

R. De Marco, Z.-T. Jiang, D. John, M. Sercombe, B. Kinsella, An in situ electrochemical impedance spectroscopy/ synchrotron radiation grazing incidence x-ray diffraction study of the influence of acetate on the carbon dioxide corrosion of mild steel, *Electrochim. Acta,* 52, 3746-3750, (2007).

A. Dick, E.R. Krausz, K.S. Hadler, C.J. Noble, P.L.W. Tregenna-Piggott and M.J. Riley, The Jahn-Teller Effect in Cu(II) Doped MgO, *J. Phys. Chem. C,* 112, 14555-14562, (2008).

B. Dittrich, C.B. Hubschle, J.J. Holstein and F.P.A. Fabbiani, Towards extracting the charge density from normal-resolution data, *J. App. Cryst.,* 42, 1110-1121, (2009).

F. Djurabekova, M. Backman, O.H. Pakarinen, K. Nordlund, L.L. Araujo and M.C. Ridgway, Amorphization of Ge nanocrystals embedded in amorphous silica under ion irradiation, *Nucl. Instrum. Meth. B,* 267, 1235-1238, (2009).

R. Dowd, G. LeBlanc and K. Zingre, Commissioning and operation of the 500 MHz storage ring RF system for the Australian Synchrotron, *Nucl. Instrum. Meth. A,* 592, 224-229, (2008).

N. Drinkwater, C.L. Gee, M. Puri, K.R. Criscione, M.J. McLeish, G.L. Grunewald, J.L. Martin, Molecular recognition of physiological substrate noradrenaline by the adrenaline-synthesizing enzyme PNMT and factors influencing its methyltransferase activity, *Biochem J.,* 422, 463-471, (2009).

X. Duan, N.H. Tran, N.K. Roberts, R.N. Lamb, Single-source chemical vapor deposition of clean oriented Al2O3 thin films, *Thin Solid Films,* 517, 6726-6730, (2009).

P. Dumas, L.M. Miller and M.J. Tobin, Challenges in Biology and Medicine with Synchrotron Infrared Light, *Acta Phys. Pol. A,* 115, 446-454, (2009).

M.B. Duriska, S.M. Neville, J. Lu, S.S. Iremonger, J.F. Boas, C.J. Kepert and S.R. Batten, Systematic Metal Variation and Solvent and Hydrogen-Gas Storage in Supramolecular Nanoballs, *Angew. Chem. Int. Edit.,* 48, 8919-8922, (2009).

M.B. Duriska, S.M. Neville, B. Moubaraki, J.D. Cashion, G.J. Halder, K.W. Chapman, C. Balde, J.F. Létard, K.S. Murray, C.J. Kepert, S.R. Batten, A Nanoscale Molecular Switch Triggered by Thermal, Light, and Guest Perturbation, *Angew. Chem. Int. Edn.,* 48, 2549-2552, (2009).

W.S. Eu, W.H. Cheung and M. Valix, Design and application of a high-temperature microfurnace for an in situ x-ray diffraction study of phase transformation, *J. Synchrotron Radiat.,* 16, 842-848, (2009).

L. Fan, D. Paterson, I. McNulty, M.M.J. Treacy and J.M. Gibson, Fluctuation x-ray microscopy: a novel approach for the structural study of disordered materials, *J. Microsc. - Oxf.,* 225, 41-48, (2007).

M.P. Fewell and J.M. Priest, High-order diffractometry of expanded austenite using synchrotron radiation, *Surf. Coat. Tech.,* 202, 1802-1815, (2008).

M.S. Gadd, D.B. Langley, J.M. Guss and J.M. Matthews, Crystallization and diffraction of an Lhx4-Isl2 complex, *Acta Crystallogr. F,* 65, 151-153, (2009).

G.J. Gainsford, S.P.H. Mee and A. Luxenburger, 'Segmented' crystals solved using synchrotron radiation: (2S,3R,4S,5R)-4-(10,10-dimethyl-3,3-dioxo-3lambda(^6)-thia-4-azatricyclo[5.2.1.0(^1,5)]decan-4-yl-carbonyl)-2,6-diphenylperhydro-pyrrolo[3,4-c]pyrrole-1,3-dione, *Acta Crystallogr. C,* 65, o331-o334, (2009).

Publications and Presentations 2007 - 2009

G.J. Gainsford, M. Delower, H. Bhuiyan and A.J. Kay, 5-(4-Cyano-5-dicyanomethylene-2,2-dimethyl-2,5-dihydro-3-furyl)-3-(1-methyl-1,4-dihydropyridin-4-ylidene)-pent-4-enyl 3,5-bis(benzyloxy)benzoate acetonitrile 0.25-solvate: a synchrotron radiation study, *Acta Crystallogr. E,* 65, o3261-o3262, (2009).

R. Giulian, L.L. Araujo, P. Kluth, D.J. Sprouster, C.S. Schnohr, B. Johannessen, G.J. Foran and M.C. Ridgway, The influence of annealing conditions on the growth and structure of embedded Pt nanocrystals, *J. Appl. Phys.,* 105, 044303, (2009).

R. Giulian, L.L. Araujo, P. Kluth, D.J. Sprouster, C.S. Schnohr, G.J. Foran and M.C. Ridgway, Temperature-dependent EXAFS analysis of embedded Pt nanocrystals, *J. Phys. - Condens. Mat.,* 21, 155302, (2009).

J.L. Glover and C.T. Chantler, The analysis of x-ray absorption fine structure: beam-line independent interpretation, *Meas. Sci. Technol.,* 18, 2916-2920, (2007).

J. L. Glover, C. T. Chantler, Z. Barnea, N. A. Rae, C. Q. Tran, D. C. Creagh, D. Paterson and B. B. Dhal, Measurements of the x-ray mass-attenuation coefficient and imaginary component of the form factor of copper, *Phys. Rev. A,* 78, 052902, (2008).

J.L. Glover, C.T. Chantler, M.D. de Jonge, Nano-roughness in gold revealed from x-ray signature, *Phys. Lett. A,* 373, 1177-1180, (2009).

J. L. Glover and C. T. Chantler, A method to determine the absolute harmonic content of an x-ray beam using attenuation measurements, *x-ray Spectrom.,* 38, 510-512, (2009).

S.W. Goh, A.N. Buckley, B. Gong, R. Woods, R.N. Lamb, L.-J. Fan, Y.-w. Yang, Thiolate layers on metal sulfides characterised by XPS, ToF-SIMS and NEXAFS spectroscopy, *Miner. Eng.,* 21, 1026-1037, (2008).

A.L. Goodwin, B.J. Kennedy, C.J. Kepert, Thermal Expansion Matching via Framework Flexibility in Zinc Dicyanometallates, *J. Am. Chem. Soc.,* 131, 6334-6335, (2009).

M. Gräfe, B. Singh, M. Balasubramanian, Surface speciation of Cd(II) and Pb(II) on kaolinite by XAFS spectroscopy, *J. Colloid Interf. Sci.,* 315, 21-32, (2007).

S. Granville, B.J. Ruck, A.R.H. Preston, T. Stewart, F. Budde, H.J. Trodahl, A. Bittar, J.E. Downes and M.C. Ridgway, Electronic properties of (Ga,Mn)N thin films with high Mn content, *J. Appl. Phys.,* 104, 103710, (2008).

S. Gras, S.R. Burrows, L. Kjer-Nielsen, C.S. Clements, Y.C. Liu, L.C. Sullivan, M.J. Bell, A.G. Brooks, A.W. Purcell, J. McCluskey and J. Rossjohn, The shaping of T cell receptor recognition by self-tolerance, *Immunity,* 30, 193-203, (2009).

K.S. Hadler, E.A. Tanifum, S.H.-C. Yip, N. Mitic, L.W. Guddat, C.J. Jackson, L.R. Gahan, K. Nguyen, P.D. Carr, D.L. Ollis, A.C. Hengge, J.A. Larrabee and G. Schenk, Substrate-Promoted Formation of a Catalytically Competent Binuclear Center and Regulation of Reactivity in a Glycerophosphodiesterase from Enterobacter aerogenes, *J. Am. Chem. Soc.,* 130, 14129-14138, (2008).

M.D. Hall, C.K. Underwood, T.W. Failes, G.J. Foran and T.W. Hambley, Using XANES to Monitor the Oxidation State of Cobalt Complexes, *Aust. J. Chem.,* 60, 180-183, (2007).

S.L. Harmer, W.M. Skinner, A.N. Buckley and L-J. Fan, Species formed at cuprite fracture surfaces; observation of O 1s surface core level shift, *Surf. Sci.,* 603, 537-545, (2009).

R.G. Haverkamp, A.T. Marshall, The mechanism of metal nanoparticle formation in plants: limits on accumulation, *J. Nanopart. Res.,* 11, 1453-1463, (2009).

R.G. Haverkamp and K.S. Wallwork, x-ray pair distribution function analysis of nanostructured materials using a Mythen detector, *J. Synchrotron Radiat.,* 16, 849-856, (2009).

J. Healy, G.H. Edward and R.B. Knott, Residual orientation in micro-injection molded parts, *J. App. Cryst.,* 40, s393-s396, (2007).

P. Heraud, M.J. Tobin, The emergence of biospectroscopy in stem cell research, *Stem Cell Res.,* 3, 12-14, (2009).

G.M. Hettiarachchi, M.J. McLaughlin, K.G. Scheckel, D.J. Chittleborough, M. Newville, S. Sutton, E. Lombi, Evidence for Different Reaction Pathways for Liquid and Granular Micronutrients in a Calcareous Soil, *Soil Sci. Soc. Am. J.,* 72, 98-110, (2008).

A.N. Hodder, R.L. Malby, O.B. Clarke, W.D. Fairlie, P.M. Colman, B.S. Crabb and B.J. Smith, Structural Insights into the Protease-like Antigen Plasmodium falciparum SERA5 and Its Noncanonical Active-Site Serine, *J. Mol. Biol.,* 392, 154-165, (2009).

Z.S. Hussain, E. Wendler, W. Wesch, G.J. Foran, C.S. Schnohr, D.J. Llewellyn and M.C. Ridgway, Rapid ion-implantation-induced amorphization of In(x)Ga(1-x)As relative to InAs and GaAs, *Phys.Rev. B,* 79, 085202, (2009).

M. Ionescu, N.P. Bhatia, D.D. Cohen, A. Kachenko, R. Siegele, M.A. Marcus, S. Fakra and G. Foran, x-ray absorption spectroscopy at the Ni-K edge in Stackhousia tryonii Bailey hyperaccumulator, *X-Ray Spectrom.,* 37, 629-634, (2008).

C.J. Jackson, M.C. Taylor, D.B. Tattersall, N.G. French, P.D. Carr, D.L. Ollis, R.J. Russell and J.G. Oakeshott, Cloning, expression, purification, crystallization and preliminary x-ray studies of a pyridoxine 50-phosphate oxidase from Mycobacterium smegmatis, *Acta Crystallogr. F,* 64, 435-437, (2008).

M. James, M. Avdeev, P. Barnes, L. Morales, K. Wallwork, R. Withers, Orthorhombic superstructures within the rare earth strontium-doped cobaltate perovskites: Ln(1-x)Sr(x)CoO(3-delta) (Ln = Y(3+), D(y3+) –Yb(3+); 0.750 <= x <= 0.875), *J. Solid State Chem.,* 180, 2233-2247, (2007).

Publications and Presentations 2007 - 2009

V. James, Fiber diffraction of skin and nails provides an accurate diagnosis of malignancies, *Int. J. Cancer,* 125, 133-138, (2009).

B. Johannessen, P. Kluth, D.J. Llewellyn, G.J. Foran, D.J. Cookson, M.C. Ridgway, Amorphization of embedded Cu nanocrystals by ion irradiation, *Appl. Phys. Lett.,* 90, 073119, (2007).

B. Johannessen, P. Kluth, D.J. Llewellyn, G.J. Foran, D.J. Cookson, M.C. Ridgway, Ion-irradiation-induced amorphization of Cu nanoparticles embedded in SiO2, *Phys. Rev. B,* 76, 184203, (2007).

A.M. Jones, R.N. Collins, J. Rose and T.D. Waite, The effect of silica and natural organic matter on the Fe(II)-catalysed transformation and reactivity of Fe(III) minerals, *Geochim. Cosmochim. Ac.,* 73, 4409-4422, (2009).

F. Jones, P. Jones, R. De Marco, B. Pejcic, A.L. Rohl, Understanding barium sulfate precipitation onto stainless steel, *Appl. Surf. Sci.,* 254, 3459-3468, (2008).

R.C. Jones, A.J. Canty, J.A. Deverell, M.G. Gardiner, R.M. Guijt, T. Rodemann, J.A. Smith, V.A. Tolhurst, Supported palladium catalysis using a heteroleptic 2-methylthiomethylpyridine-N,S-donor motif for Mizoroki-Heck and Suzuki-Miyaura coupling, including continuous organic monolith in capillary microscale flow-through mode, *Tetrahedron,* 65, 7474-7481, (2009).

H.J. Kang, N.G. Paterson, A.H. Gaspar, H. Ton-That, and E.N. Baker, The Corynebacterium diphtheriae shaft pilin SpaA is built of tandem Ig-like modules with stabilizing isopeptide and disulfide bonds, *P. Natl. Acad. Sci. U.S.A.,* 106, 16967-16971, (2009).

H.J. Kang, N.G. Paterson and E.N. Baker, Expression, purification, crystallization and preliminary crystallographic analysis of SpaA, a major pilin from Corynebacterium diphtheriae, *Acta Crystallogr. F,* 65, 802-804, (2009).

N. Kaur, M. Gräfe, B. Singh, B. Kennedy, Simultaneous incorporation of Cr, Zn, Cd, and Pb in the goethite structure, *Clay. Clay Miner.,* 57, 234-250, (2009).

N. Kaur, B. Singh, B.J. Kennedy, M. Gräfe, The preparation and characterization of vanadium-substituted goethite: The importance of temperature, *Geochim. Cosmochim. Ac.,* 73, 582-593, (2009).

B.J. Kennedy and P.J. Saines, Phase segregation in mixed Nb-Sb double perovskites Ba2LnNb(1-x)Sb(x)O6, *J. Solid State Chem.,*181, 298-305, (2008).

B.J. Kennedy and Q. Zhou, The role of orbital ordering in the tetragonal-to-cubic phase transition in CuCr2O4, *J. Solid State Chem.,* 181, 2227-2230, (2008).

B.J. Kennedy, P.J. Saines, Q. Zhou, Z. Zhang, M. Matsuda and M. Miyake, Structural and electronic phase transitions in Sr(1-x)Ce(x)MnO3 perovskites, *J. Solid State Chem.,* 181, 2639-2645, (2008).

B.J. Kennedy and Q. Zhou, Sequential Jahn-Teller and Tilting Transitions in the Mixed Ru Mn Perovskite SrRu(0.5)Mn(0.5) O3, *Solid State Commun.,* 147, 208-211, (2008).

B.J. Kennedy, Q. Zhou, Ismunandar, Y. Kubota, K. Kato, Cation disorder and phase transitions in the four-layer ferroelectric Aurivillius phases ABi4Ti4O15 (A = Ca, Sr, Ba, Pb), *J. Solid State Chem.,* 181, 1377-1386, (2008).

B.J. Kennedy, J. Ting, Q. Zhou, Z. Zhang, M. Matsuda and M. Miyake, Structural Characterisation of the Perovskite Series Sr(0.9-x)Ca(x)Ce(0.1)MnO3: Influence of the Jahn-Teller Effect, *J. Solid State Chem.,* 182, 954-959, (2009).

B.J. Kennedy, P.J. Saines, J. Ting, Q. Zhou, J.A. Kimpton, Structural characterisation of the perovskite series Sr(x)Ca(1-x-y)Nd(y)MnO3: Influence of the Jahn–Teller effect, *J. Solid State Chem.,* 182, 2858-2866, (2009).

B. Kent, C.J. Garvey, D. Cookson, G. Bryant, The inverse hexagonal - inverse ribbon - lamellar gel phase transition sequence in low hydration DOPC:DOPE phospholipid mixtures, *Chem. Phys. Lipids.,* 157, 56-60, (2009).

N. Kirby, D. Cookson, C. Buckley, E. Bovell and T. St Pierre, Iron K-edge anomalous small-angle x-ray scattering at 15-ID-D at the Advanced Photon Source, *J. App. Cryst.,* 40, s402-s407, (2007).

P. Kluth, B. Hoy, B. Johannessen, S.G. Dunn, G.J. Foran, D.J. Cookson, M.C. Ridgway, Formation and characterization of nanoparticles formed by sequential ion implantation of Au and Co into SiO2, *Nucl. Instrum. Meth. B,* 257, 80-84, (2007).

P. Kluth, B. Johannessen, R. Giulian, C.S. Schnohr, G.J. Foran, D.J. Cookson, A.P. Byrne and M.C. Ridgway, Ion irradiation effects on metallic nanocrystals, *Radiat. Eff. Defects Solids,* 162, 501-513, (2007).

P. Kluth, C.S. Schnohr, O.H. Pakarinen, F. Djurabekova, D.J. Sprouster, R. Giulian, M.C. Ridgway, A.P. Byrne, C. Trautmann, D.J. Cookson, K. Nordlund and M. Toulemonde, Fine Structure in Swift Heavy Ion Tracks in Amorphous SiO2, *Phys. Rev. Lett.,* 101, 175503, (2008).

P. Kluth, R. Giulian, D.J. Sprouster, C.S. Schnohr, A.P. Byrne, D.J. Cookson and M.C. Ridgway, Energy dependent saturation width of swift heavy ion shaped embedded Au nanoparticles, *Appl. Phys. Lett.,* 94, 113107, (2009).

A. Kohler, J. Sule-Suso, G.D. Sockalingum, M. Tobin, F. Bahrami, Y. Yang, J. Pijanka, P. Dumas, M. Cotte, D.G. van Pittius, G. Parkes and H. Martens, Estimating and Correcting Mie Scattering in Synchrotron-Based Microscopic Fourier Transform Infrared Spectra by Extended Multiplicative Signal Correction, *Appl. Spectrosc.,* 62, 259-266, (2008).

E.F. Lee, P.E. Czabotar, H. Yang, B.E. Sleebs, G. Lessene, P.M. Colman, B.J. Smith and W.D. Fairlie, Conformational Changes in Bcl-2 Pro-survival Proteins Determine Their Capacity to Bind Ligands, *J. Biol. Chem,* 284, 30508-30517, (2009).

Publications and Presentations 2007 - 2009

V. Lee, D.J. Peake, B. Sobott, B. Schroder, Ch. Bronnimann, B. Henrich, K. Hansen, G.J. O'Keefe, G.N. Taylor, M.J. Boland, M.N. Thompson, R.P. Rassool, Imaging high energy photons with PILATUS II at the tagged photon beam at MAX-lab, *Nucl. Instrum. Meth. A,* 603, 379-383, (2009).

A. Levina, H.H. Harris and P.A. Lay, X-Ray Absorption and EPR Spectroscopic Studies of the Biotransformations of Chromium(VI) in Mammalian Cells. Is Chromodulin an Artifact of Isolation Methods?, *J. Am. Chem. Soc.,* 129, 1065-1075, (2007).

A. Levina, A.I. McLeod, J. Seuring, P.A. Lay, Reactivity of potential anti-diabetic molybdenum(VI) complexes in biological media: A XANES spectroscopic study, *J. Inorg. Biochem.,* 101, 1586-1593, (2007).

A. Levina, and P.A. Lay, Chemical Properties and Toxicity of Chromium(III) Nutritional Supplements, *Chem. Res. Toxicol.,* 21, 563-571, (2008).

A. Levina, A. Mitra, P.A. Lay, Recent developments in ruthenium anticancer drugs, *Metallomics,* 1, 458-470, (2009).

J. Li, D.J. Cookson and A.R. Gerson, Crystal Growth through Progressive Densification Identified by Synchrotron Small-Angle x-ray Scattering, *Cryst. Growth Des.,* 8, 1730-1733, (2008).

C.D. Ling, M. Avdeev and K. Aivazian, Synthesis, structure, and stability of the high-temperature 6H-type perovskite phase Ba3BaSb2O9, *Acta Crystallogr. B,* 63, 584-588, (2007).

C.D. Ling, K. Aivazian, S.A. Schmid and P. Jensen, Structural investigation of oxygen non-stoichiometry and cation doping in misfit-layered thermoelectric (Ca2CoO[3-x])(CoO2)delta, delta ~ 1.61, *J. Solid State Chem.,* 180, 1446-1455, (2007).

C.D. Ling, M. Avdeev, R. Kutteh, V.V. Kharton, A.A. Yaremchenko, S. Fialkova, N. Sharma, R.B. Macquart, M. Hoelzel, and M. Gutmann. Structures, phase transitions, hydration and ionic conductivity of Ba4Nb2O9, *Chem. Mater.,* 21, 3853-3864, (2009).

C. Linke, T.T. Caradoc-Davies, T. Proft and E.N. Baker, Purification, crystallization and preliminary crystallographic analysis of Streptococcus pyogenes laminin-binding protein Lbp, *Acta Crystallogr. F,* 64, 141-143, (2008).

C. Linke, T.T. Caradoc-Davies, P.G. Young, T. Proft and E.N. Baker, The Laminin-Binding Protein Lbp from Streptococcus pyogenes Is a Zinc Receptor, *J. Bacteriology,* 191, 5814-5823, (2009).

W. Liu, B. Etschmann, G. Foran, M. Shelley and J. Brugger, Deriving formation constants for aqueous metal complexes from XANES spectra: Zn(2+) and Fe(2+) chloride complexes in hypersaline solutions, *Am. Mineral.,* 92, 761-770, (2007).

M. Lopez, B. Paul, A. Hofmann, J. Morizzi, Q.K. Wu, S.A. Charman, A. Innocenti, D. Vullo, C.T. Supuran and S.-A. Poulsen, S-Glycosyl Primary Sulfonamides-A New Structural Class for Selective Inhibition of Cancer-Associated Carbonic Anhydrases, *J. Med. Chem.,* 52, 6421-6432, (2009).

I.M. Low, E. Wren, K.E. Prince A. Atanacio, Characterisation of phase relations and properties in air-oxidised Ti3SiC2, *Materi. Sci. Eng. A.,* 466, 140-147, (2007).

I.M. Low, Z. Oo, K.E. Prince, Effect of Vacuum Annealing on the Phase Stability of Ti3SiC2, *J. Am. Ceram. Soc.,* 90, 2610-2614, (2007).

I.M. Low, N. Duraman, U. Mahmood, Mapping the structure, composition and mechanical properties of human teeth, *Mater. Sci. Eng. C - Mater. Biol. Appl.,* 28, 243-247, (2008).

J. Lu, D.R. Turner, L.P. Harding, L.T. Byrne, M.V. Baker and S.R. Batten. Octapi Interactions: Self-Assembly of a Pd-Based [2]Catenane Driven by Eightfold Pi-Interactions, *J. Am. Chem. Soc.,* 131, 10372-10373, (2009).

V. Luca, Comparison of Size-Dependent Structural and Electronic Properties of Anatase and Rutile Nanoparticles, *J. Phys. Chem. C,* 113, 6367-6380, (2009).

V. Luca, W.K. Bertram, G.D. Sizgek, B. Yang and D. Cookson, Delineating the First Few Seconds of Supramolecular Self-Assembly of Mesostructured Titanium Oxide Thin Films through Time-Resolved Small Angle x-ray Scattering, *Langmuir,* 24, 10737-10745, (2008).

J. Ma, G.P. Simon and G.H. Edward, The Effect of Shear Deformation on Nylon-6 and Two Types of Nylon-6/Clay Nanocomposite, *Macromolecules,* 41, 409-420, (2008).

W.A. Macdonald, Z. Chen, S. Gras, J.K. Archbold, F.E. Tynan, C.S. Clements, M. Bharadwaj, L. Kjer-Nielsen, P.M. Saunders, M.C.J. Wilce, F. Crawford, B. Stadinsky, D. Jackson, A.G. Brooks, A.W. Purcell, J.W. Kappler, S.R. Burrows, J. Rossjohn and J. McCluskey, T cell allorecognition via Molecular Mimicry, *Immunity,* 31, 897-908, (2009).

C.R. McNeill, B. Watts, L. Thomsen, W.J. Belcher, N.C. Greenham, P.C. Dastoor and H. Ade, Evolution of Laterally Phase-Separated Polyfluorene Blend Morphology Studied by x-ray Spectromicroscopy, *Macromolecules,* 42, 3347-3352, (2009).

E. Meier, S.G. Biedron, G. LeBlanc, M.J. Morgan, J. Wue, Development of a combined feed forward-feedback system for an electron Linac, *Nucl. Instrum. Meth. A,* 609, 79-88, (2009).

E. Meier, S.G. Biedron, G. LeBlanc, M.J. Morgan, J. Wu, Electron beam energy and bunch length feed forward control studies using an artificial neural network at the Linac coherent light source, *Nucl. Instrum. Meth. A,* 610, 629-635, (2009).

E. Meier, R. Dowd and G. LeBlanc, Characterization of the Australian Synchrotron Linac, *Nucl. Instrum. Meth. A,* 589, 157-166, (2008).

Publications and Presentations 2007 - 2009

M. Minakshi, D.R.G. Mitchell, M.L. Carter, D. Appadoo, K. Nallathamby, Microstructural and spectroscopic investigations into the effect of CeO2 additions on the performance of a MnO2 aqueous rechargeable battery, *Electrochim. Acta,* 54, 3244-3249, (2009).

N. Mitik-Dineva, J. Wang, V.K. Truong, P.R. Stoddart, F. Malherbe, R.J. Crawford and E.P. Ivanova, Differences in colonisation of five marine bacteria on two types of glass surfaces, *Biofouling,* 25, 621-631, (2009).

A.M. Mulders, S.M. Lawrence, U. Staub, M. Garcia-Fernandez, V. Scagnoli, C. Mazzoli, E. Pomjakushina, K. Conder, Y. Wang, Direct observation of charge order and orbital glass state in multiferroic LuFe2O4., *Phys. Rev. Lett.,* 103, 077602, (2009).

X. Mulet, X. Gong, L.J. Waddington, C.J. Drummond, Observing Self-Assembled Lipid Nanoparticles Building Order and Complexity through Low-Energy Transformation Processes, *ACS Nano,* 3, 2789-2797, (2009).

K.L. Munro, A. Mariana, A.I. Klavins, A.J. Foster, B. Lai, S. Vogt, Z. Cai, H.H. Harris and C.T. Dillon, Microprobe XRF Mapping and XAS Investigations of the Intracellular Metabolism of Arsenic for Understanding Arsenic-Induced Toxicity, *Chem. Res. Toxicol.,* 21, 1760-1769, (2008).

A. Nafady, A.M. Bond, A. Bilyk A.R. Harris, A.I. Bhatt, A.P. O'Mullane and R. De Marco, Tuning the Electrocrystallization Parameters of Semiconducting Co[TCNQ]2-Based Materials To Yield either Single Nanowires or Crystalline Thin Films, *J. Am. Chem. Soc.,* 129, 2369-2382, (2007).

K.M. Nairn, R.E. Lyons, R.J. Mulder, S.T. Mudie, D.J. Cookson, E. Lesieur, M. Kim, D. Lau, F.H. Scholes and C.M. Elviny, A Synthetic Resilin Is Largely Unstructured, *Biophys. J.,* 95, 3358-3365, (2008).

P. Nel, A preliminary investigation into the identification of adhesives on archaeological pottery, *AICCM Bulletin,* 30, 27-37, (2007).

J. Newman, E.H. Cohen, L. Cosgrove, K. Kopacz, D.T. Dransfield, T.E. Adams and T.S. Peat, Crystallization and preliminary x-ray analysis of the complexes between a Fab and two forms of human insulin-like growth factor II, *Acta Crystallogr. F,* 65, 945-948, (2009).

J. Newman, V.J. Fazio, T.T. Caradoc-Davies, K. Branson, T.S. Peat, Practical Aspects of the SAMPL Challenge: Providing an Extensive Experimental Data Set for the Modeling Community, *J. Biomol. Screen.,* 14, 1245-1250, (2009).

A. Nguyen, I. Mulyani, A. Levina, and P.A. Lay, Reactivity of Chromium(III) Nutritional Supplements in Biological Media: An X-Ray Absorption Spectroscopic Study, *Inorg. Chem.,* 47, 4299-4309, (2008).

A.J. Oakley, T. Yamada, D. Liu, M. Coggan, A.G. Clark and P.G. Board, The Identification and Structural Characterization of C7orf24 as gamma-Glutamyl Cyclotransferase: an essential enzyme in the gamma-glutamyl cycle, *J. Biol. Chem.,* 283, 22031-22042, (2008).

H.St.C. O'Neill, A.J. Berry, S.M. Eggins, The solubility and oxidation state of tungsten in silicate melts: Implications for the comparative chemistry of W and Mo in planetary differentiation processes, *Chem. Geol.,* 255, 346-359, (2008).

W.K. Pang, I.M. Low, B.H. O'Connor, A.J. Studer, V.K. Peterson and J.-P. Palmquist, Effect of Vacuum Annealing on the Thermal Stability of Ti3SiC2/TiC/TiSi2 Composites, *J. Aust. Ceram. Soc.,* 45, 72-77, (2009).

W.K. Pang, I.M. Low and J.V. Hanna, Detection of Amorphous Silica in Air-Oxidized Ti3SiC2 at 500 - 1000 degC, *J. Aust. Ceram. Soc.,* 45, 39-43, (2009).

W.K. Pang and I.M. Low, Diffraction Study of Thermal Dissociation in the Ternary Ti-Al-C System, *J. Aust. Ceram. Soc.,* 45, 30-33, (2009).

W.K. Pang, I.M. Low, B.H. O'Connor, Z.M. Sun and K.E. Prince, Oxidation characteristics of Ti3AlC2 over temperature range 500-900 degC, *Mater. Chem. Phys.,* 117, 384-389, (2009).

D.J. Peake, M.J. Boland, G.S. LeBlanc and R.P. Rassool, Measurement of the real time fill-pattern at the Australian Synchrotron, *Nucl. Instrum. Meth. A,* 589, 143-149, (2008).

D.G. Pellicci, O. Patel, L. Kjer-Nielsen, S.S. Pang, L.C. Sullivan, K. Kyparissoudis, A.G. Brooks, H.H. Reid, S. Gras, I.S. Lucet, R. Koh, M.J. Smyth, T. Mallevaey, J.L. Matsuda, L. Gapin, J. McCluskey, D.I. Godfrey and J. Rossjohn, Differential Recognition of CD1d-alpha-Galactosyl Ceramide by the V beta 8.2 and V beta 7 Semi-invariant NKT T Cell Receptors, *Immunity,* 31, 47-59, (2009).

B. Pemberton and P. Nel, Identification of a white substance on 20th century leather bindings, *AICCM Bulletin,* 31, 28-35, (2008).

N.R. Pendini, S.W. Polyak, G.W. Booker, J.C. Wallace and M.C.J. Wilce, Purification, crystallization and preliminary crystallographic analysis of biotin protein ligase from Staphylococcus aureus, *Acta Cryst. F,* 64, 520-523, (2008).

K.C. Prince, V. Feyer, A. Tadich, L. Thomsen and B.C.C. Cowie, Photoabsorption and photoemission of magnesium diboride at the Mg K edge, *J. Phys. - Condens. Mat.,* 21, 405701, (2009).

I. Quesada-Soriano, L.J. Parker, A. Primavera, J.M. Casas-Solvas, A. Vargas-Berenguel, C. Barón, C.J. Morton, A.P. Mazzetti, M. Lo Bello, M.W. Parker and L. García-Fuentes, Influence of the H-site residue 108 on human glutathione transferase P1-1 ligand binding: Structure-thermodynamic relationships and thermal stability, *Protein Sci.,* 18, 2454-2470, (2009).

Publications and Presentations 2007 - 2009

A.P. Radlinski, T.L. Busbridge, E. Mac A. Gray, T.P. Blach, D.J. Cookson, Small angle x-ray scattering mapping and kinetics study of sub-critical CO2 sorption by two Australian coals, *Int. J. Coal Geol.,* 77, 80-89, (2009).

A.P. Radlinski, T.L. Busbridge, E.MacA. Gray, T.P. Blach, G. Cheng, Y.B. Melnichenko, D.J. Cookson, M. Mastalerz and J. Esterle, Dynamic Micromapping of CO2 Sorption in Coal, *Langmuir,* 25, 2385-2389, (2009).

M.C. Ridgway, P. Kluth, R. Giulian, D.J. Sprouster, L.L. Araujo, C.S. Schnohr, D.J. Llewellyn, A.P. Byrne, G.J. Foran and D.J. Cookson, Changes in metal nanoparticle shape and size induced by swift heavy-ion irradiation, *Nucl. Instrum. Meth. B,* 267, 931-935, (2009).

E.G. Robertson, C. Medcraft, L. Puskar, R. Tuckermann, C.D. Thompson, S. Bauerecker and D. McNaughton, IR spectroscopy of physical and chemical transformations in cold hydrogen chloride and ammonia aerosols, *Phys. Chem. Chem. Phys.,* 11, 7853-7860, (2009).

R.L. Ryall, P.K. Grover, L.A. Thurgood, M.C. Chauvet, D.E. Fleming, W. van Bronswijk, The importance of a clean face: the eVect of diVerent washing procedures on the association of Tamm–Horsfall glycoprotein and other urinary proteins with calcium oxalate crystals, *Urol. Res.,* 35, 1-14, (2007).

S.M. Sagnella, C.E. Conn, I. Krodkiewska and C.J. Drummond, Soft ordered mesoporous materials from nonionic isoprenoid-type monoethanolamide amphiphiles self-assembled in water, *Soft Matter,* 5, 4823-4834, (2009). "

P.J. Saines, J.R. Spencer, B.J. Kennedy, M. Avdeev, Structures and crystal chemistry of the double perovskites Ba2LnB'O6 (Ln = lanthanide B' = Nb[5+] and Ta[5+]): Part I. Investigation of Ba2LnTaO6 using synchrotron x-ray and neutron powder diffraction, *J. Solid State Chem.,* 180, 2991-3000, (2007).

P.J. Saines, J.R. Spencer, B.J. Kennedy, Y. Kubota, C. Minakata, H. Hano, K. Kato, M. Takata, Structures and crystal chemistry of the double perovskites Ba2LnB'O6 (Ln = lanthanide and B' = Nb, Ta): Part II-Temperature dependence of the structures of Ba2LnB'O6, *J. Solid State Chem.,* 180, 3001-3007, (2007).

P.J. Saines, B.J. Kennedy, M.M. Elcombe, Structural phase transitions and crystal chemistry of the series Ba2LnB'O6 (Ln = lanthanide and B' = Nb[5+] or Sb[5+]), *J.Solid State Chem.,* 180, 401-409, (2007).

P.J. Saines, B.J. Kennedy, B. Johannessen and S. Poulton, Phase and Valence State Transitions in Ba2LnSnxNb1-xO6-delta, *J. Solid State Chem.,* 181, 2994-3004, (2008).

P.J. Saines, B.J. Kennedy, M.M. Elcombe, H.H. Harris, L-Y. Jang and Z. Zhang, Phase and valence transitions in Ba2LnSn(x)Sb(1-x)O(6-delta) (Ln = Pr and Tb), *J. Solid State Chem.,* 181, 2941-2952, (2008).

P.J. Saines, B.J. Kennedy and R.I. Smith, Structural Phase Transitions in BaPrO3, *Mater. Res. Bull.,* 44, 874-879, (2009).

P.S. Salamakha, O.L. Sologub, J.R. Hester, C. Rizzoli, A.P. Goncalves, M. Almeida, Rietveld refinement of the RNi4B compounds (R = Gd, Tb, Er), *J. Alloy. Compd.,* 439, 162-165, (2007).

A.J. Scardino, H. Zhang, D.J. Cookson, R.N. Lamb, R. de Nys, The role of nano-roughness in antifouling, *Biofouling,* 25, 757-767, (2009).

G. Schenk, R.A. Peralta, S.C. Batista, A.J. Bortoluzzi, B. Szpoganicz, A.K. Dick, P. Herrald, G.R. Hanson, R.K. Szilagyi, M.J. Riley, L.R. Gahan, A. Neves, Probing the role of the divalent metal ion in uteroferrin using metal ion replacement and a comparison to isostructural biomimetics, *J. Biol. Inorg. Chem.,* 13, 139-155, (2008).

C.S. Schnohr, P. Kluth, A.P. Byrne, G.J. Foran and M.C. Ridgway, EXAFS study of the amorphous phase of InP after swift heavy ion irradiation, *Nucl. Instrum. Meth. B,* 257, 293-296, (2007).

C.S. Schnohr, L.L. Araujo, P. Kluth, D.J. Sprouster, G.J. Foran, M.C. Ridgway, Atomic-scale structure of Ga(1-x)In(x) P measured with extended x-ray absorption fine structure spectroscopy, *Phys. Rev. B,* 78, 115201, (2008).

T. Sercombe, N. Jones, R. Day and A. Kop, Heat treatment of Ti-6Al-7Nb components produced by selective laser melting, *Rapid Prototyping J.,* 14, 300-304, (2008).

P. Shah, V. Strezov, C. Stevanov, P.F. Nelson, Speciation of Arsenic and Selenium in Coal Combustion Products, *Energ. Fuel.,* 21, 506-512, (2007).

P. Shah, V. Strezov, K. Prince, P.F. Nelson, Speciation of As, Cr, Se and Hg under coal fired power station conditions, *Fuel,* 87,1859-1869, (2008).

P. Shah, V. Strezov, P.F. Nelson, X-Ray Absorption Near Edge Structure Spectrometry Study of Nickel and Lead Speciation in Coals and Coal Combustion Products, *Energ. Fuel.,* 23, 1518-1525, (2009).

N. Sharma, R.L. Withers, K.S. Knight, and C.D. Ling, Structure, crystal chemistry, and thermal evolution of the delta-Bi2O3-related phase Bi9ReO17, *J. Solid State Chem.,* 182, 2468-2474, (2009).

C.J. Shearer, J. Yu, K.M. O'Donnell, L. Thomsen, P.C. Dastoor, J.S. Quinton and J.G. Shapter, Highly resilient field emission from aligned single-walled carbon nanotube arrays chemically attached to n-type silicon, *J. Mater. Chem.,* 18, 5753-5760, (2008).

S.R. Shouldice, B. Heras, R. Jarrott, P. Sharma, M.J. Scanlon and J.L. Martin, Characterization of the DsbA Oxidative Folding Catalyst from Pseudomonas aeruginosa Reveals a Highly Oxidizing Protein that Binds Small Molecules, *Antioxid. Redox Signal.,* 12, 921-931, (2009).

G.D. Sizgek, E. Sizgek, C.S. Griffith, and V. Luca, Mesoporous Zirconium Titanium Oxides. Part 2: Synthesis, Porosity, and Adsorption Properties of Beads, *Langmuir,* 24, 12323-12330, (2008).

Publications and Presentations 2007 - 2009

S.J. Smith, A. Casellato, K.S. Hadler, N. Mitic, M.J. Riley, A.J. Bortoluzzi, B. Szpoganicz, G. Schenk, A. Neves, L.R. Gahan, The reaction mechanism of the Ga(III)Zn(II) derivative of uteroferrin and corresponding biomimetics, *J. Biol. Inorg. Chem.,* 12, 1207-1220, (2007).

C. Song, R. Bergstrom, D. Ramunno-Johnson, H. Jiang, D. Paterson, M.D. de Jonge, I. McNulty, J. Lee, K.L. Wang, and J. Miao, Nanoscale Imaging of Buried Structures with Elemental Specificity Using Resonant X-Ray Diffraction Microscopy, *Phys. Rev. Lett.,* 100, 025504, (2008).

D.J. Sprouster, R. Giulian, P. Kluth, L.L. Araujo, G.J. Foran, D.J. Cookson, M.C. Ridgway, Synchrotron radiation characterisation of Cobalt nanoparticles formed by ion implantation, *Adv. Sync. Rad.,* 1, 189-196, (2008).

D. J. Sprouster, R. Giulian, C. S. Schnohr, L. L. Araujo, P. Kluth, A. P. Byrne, G. J. Foran, B. Johannessen and M. C. Ridgway, FCC-HCP phase transformation in Co nanoparticles induced by swift heavy-ion irradiation, *Phys. Rev. B,* 80, 115438, (2009).

A. Stacey, Sh. Michaelson, J. Orwa, S. Rubanov, S. Prawer, B.C.C. Cowie and A. Hoffman, Near coalescent submicron polycrystalline diamond films deposited on silicon: Hydrogen bonding and thermal enhanced carbide formation, *J. Appl. Phys.,* 106, 103503, (2009).

J. Thieme, I. McNulty, S. Vogt, D. Paterson, x-ray Spectromicroscopy - A Tool for Environmental Sciences, *Environ. Sci. Technol.,* 41, 6885-6889, (2007).

L. Thomsen, M.T. Wharmby, D.P. Riley, G. Held and M.J. Gladys, The adsorption and stability of sulphur containing amino acids on Cu{531}, *Surf. Sci.,* 603, 1253-1261, (2009).

G.J. Thorogood, B.J. Kennedy, V. Luca, M. Blackford, S.K. van de Geest, K.S. Finnie, J.V. Hanna, K.J. Pike, Structure and dehydration of the pyrochlore system NaW(2-y)MoyO(6+delta). nH(2-z)O between 10 and 675 K, *J. Phys. Chem. Solids,* 69, 1632-1640, (2008).

G.J. Thorogood, B.J. Kennedy, Ismunadar, M. Avdeev, T. Kamiyama, The stability of Na-doped Bi2(NbCr)O(7-x) pyrochlores: The non-existence of ''(BiNa)(NbCr)O6'', *J. Phys. Chem. Solids,* 69, 918-922, (2008).

G.J. Thorogood, P.J. Saines, B.J. Kennedy, R.L. Withers and M.M. Elcombe, Diffuse scattering in the cesium pyrochlore CsTi(0.5)W(1.5)O6, *Mater. Res. Bull.,* 43, 787-795, (2008).

K. Thumanu, W. Tanthanuch, C. Lorthongpanich, P. Heraud, R. Parnpai, FTIR microspectroscopic imaging as a new tool to distinguish chemical composition of mouse blastocyst, *J. Mol. Struct.,* 933, 104-111, (2009).

J. Ting, B.J. Kennedy, R.L. Withers and M. Avdeev, Synthesis and structural studies of lanthanide substituted bismuth-titanium pyrochlores, *J. Solid State Chem.,* 182, 836-840, (2009).

C.Q. Tran, G.J. Williams, A.Roberts, S. Flewett, A.G. Peele, D. Paterson, M.D. de Jonge and K.A. Nugent, Experimental Measurement of the Four-Dimensional Coherence Function for an Undulator X-Ray Source, *Phys. Rev. Lett.,* 98, 224801, (2007).

V.K. Truong, S. Rundell, R. Lapovok, Y. Estrin, J.Y. Wang, C.C. Berndt, D.G. Barnes, C.J. Fluke, R.J. Crawford, E.P. Ivanova, Effect of ultrafine-grained titanium surfaces on adhesion of bacteria, *Appl. Microbiol. Biotechnol.,* 83, 925-937, (2009).

R. Tuckermann, L. Puskar, M. Zavabeti, R. Sekine, D. McNaughton, Chemical analysis of acoustically levitated drops by Raman spectroscopy, *Anal. Bioanal. Chem.,* 394, 1433-1441, (2009).

M. Valix , W.H. Cheung, K. Zhang, Role of chemical pre-treatment in the development of super-high surface areas and heteroatom fixation in activated carbons prepared from bagasse, *Micropor. Mesopor. Mat.,* 116, 513-523, (2008).

S.C. Van Sluyter, M. Marangon, S.D. Stranks, K.A. Neilson, Y. Hayasaka, P.A. Haynes, R.I. Menz and E.J. Waters, Two-Step Purification of Pathogenesis-Related Proteins from Grape Juice and Crystallization of Thaumatin-like Proteins, *J. Agr. Food Chem.,* 57, 11376-11382, (2009).

J.P. Vivian , T. Beddoe, A.D. McAlister, M.C. Wilce, L. Zaker-Tabrizi, S. Troy, E. Byres, D.E. Hoke, P.A. Cullen, M. Lo, G.L. Murray, B. Adler, J. Rossjohn, Crystal Structure of LipL32, the Most Abundant Surface Protein of Pathogenic Leptospira spp., *J. Mol. Biol.,* 387,1229-1238, (2009).

J.E. Voss, S.W. Scally, N.L. Taylor, C. Dogovski, M.R. Alderton, C.A. Hutton, J.A. Gerrard, M.W. Parker, R.C.J. Dobson and M.A. Perugini, Expression, purification, crystallization and preliminary x-ray diffraction analysis of dihydrodipicolinate synthase from Bacillus anthracis in the presence of pyruvate, *Acta Crystallogr. F,* 65, 188-191, (2009).

G.T. Webster, K.A. de Villiers, T.J. Egan, S. Deed, L. Tilley, M.J. Tobin, K.R. Bambery, D. McNaughton and B.R. Wood, Discriminating the Intraerythrocytic Lifecycle Stages of the Malaria Parasite Using Synchrotron FT-IR Microspectroscopy and an Artificial Neural Network, *Anal. Chem.,* 81, 2516-2524, (2009).

N.A.S. Webster, C.D. Ling, C.L. Raston and F.J. Lincoln, The structure and conductivity of new fluorite-type Bi2O3-Er2O3-PbO materials, *Solid State Ionics,* 178, 1451-1457, (2007).

N.A.S. Webster, I.C. Madsen, M.J. Loan, N.V.Y. Scarlett, K.S. Wallwork, A flow cell for in situ synchrotron x-ray diffraction studies of scale formation under Bayer processing conditions, *Rev. Sci. Instrum.,* 80, 084102, (2009).

C.E. White, J.L. Provis, D.P. Riley, G.J. Kearley and J.S.J. van Deventer, What is the structure of kaolinite? Reconciling theory and experiment, *J. Phys. Chem. B,* 113, 6756 - 6765, (2009).

Publications and Presentations 2007 - 2009

G.J. Williams, H.M. Quiney, B.B. Dahl, C.Q. Tran, A.G. Peele, K.A. Nugent, M.D. De Jonge, D. Paterson, Curved beam coherent diffractive imaging, *Thin Solid Films,* 515, 5553-5556, (2007).

N.K. Williams, R.S. Bamert, O. Patel, C. Wang, P.M. Walden, A.F. Wilks, E. Fantino, J. Rossjohn and I.S. Lucet, Dissecting Specificity in the Janus Kinases: The Structures of JAK-Specific Inhibitors Complexed to the JAK1 and JAK2 Protein Tyrosine Kinase Domains, *J. Mol. Biol.,* 387, 219-232, (2009).

B.R. Wood, T. Chernenko, C. Matthaus, M. Diem, C. Chong, U. Bernhard, C. Jene, A.A. Brandli, D. McNaughton, M.J. Tobin, A. Trounson and O. Lacham-Kaplan, Shedding New Light on the Molecular Architecture of Oocytes Using a Combination of Synchrotron Fourier Transform-Infrared and Raman Spectroscopic Mapping, *Anal. Chem.,* 80, 9065-9072, (2008).

Q. Zhou, B.J. Kennedy, A variable temperature structural study of the Jahn-Teller distortion in Ba2CuUO6, *J. Phys. Chem. Solids,* 68, 1643-1647, (2007).

Q. Zhou, B.J. Kennedy, M.M. Elcombe, R.L. Withers, Composition- and temperature-dependent phase transitions in 1:3 ordered perovskites Ba(4-x)Sr(x)NaSb3O12, *J. Solid State Chem.,* 180, 3082-3092, (2007).

Q. Zhou, B.J. Kennedy, M.M. Elcombe, Composition and temperature dependent phase transitions in Co–W double perovskites, a synchrotron x-ray and neutron powder diffraction study, *J. Solid State Chem.,* 180, 541-548, (2007).

Q. Zhou, B.J. Kennedy, M. Avdeev, L. Giachini, J. Kimpton, Structural studies of the phases in Ba2LaIrO6 - New light on an old problem, *J. Solid State Chem.,* 182, 3195-3200, (2009).

Q. Zhou, P.J. Saines, N. Sharma, J.Ting, B.J. Kennedy, Z. Zhang, R.L. Withers and K.S. Wallwork, Crystal Structures and Phase Transitions in A-site deficient Perovskites Ln1/3TaO3, *Chem. Mater.,* 20, 6666-6676, (2008).

P.-W. Zhu, J. Tung, G. Edward, and L. Nichols, Effects of different colorants on morphological development of sheared isotactic polypropylene: A study using synchrotron wide-angle x-ray scattering, *J. Appl. Phys.,* 103, 124906, (2008).

P.-W. Zhu and G. Edward, Orientational distribution of parent–daughter structure of isotactic polypropylene: a study using simultaneous synchrotron WAXS and SAXS, *J. Mater. Sci.,* 43, 6459-6467, (2008).

P.-W. Zhu, G. Edward and L. Nichols, Effect of additives on distributions of lamellar structures in sheared polymer: a study of synchrotron small-angle x-ray scattering, *J. Phys. D Appl. Phys.,* 42, 245406, (2009).

P.-W. Zhu, A. Phillips, G. Edward, L. Nichols, Experimental observation of effects of seeds on polymer crystallization, *Phys. Rev. E,* 80, 051801, (2009).

C.W. Zou, X.D. Yan, J. Han, R.Q. Chen and W. Gao, Microstructures and optical properties of beta-V2O5 nanorods prepared by magnetron sputtering, *J. Phys. D Appl. Phys.,* 42, 145402, (2009).

C.W. Zou, X.D. Yan, J. Han, R.Q. Chen, W. Gao, and J. Metson, Study of a nitrogen-doped ZnO film with synchrotron radiation, *Appl. Phys. Lett.* 94, 171903, (2009).

C.W. Zou, X.D. Yan, J. Han, R.Q. Chen, J.M. Bian, E. Haemmerle, W. Gao, Preparation and enhanced photoluminescence property of ordered ZnO/TiO2 bottlebrush nanostructures, *Chem. Phys. Lett.,* 476, 84-88, (2009).

Australian Synchrotron Users

The User Office

The User Office is the first point of contact for all current and prospective users, and central to the experience associated with working at the Australian Synchrotron and producing research outcomes.

In addition to ensuring that more than 600 proposals a year are properly reviewed, ranked and awarded beamtime, the User Office sees to the practical needs of the hundreds of users who come to the Australian Synchrotron annually.

The User Office oversees the review of all merit-based proposals to use the facility, beamtime scheduling and flow of information and advice to the user community. Post-beamtime, the User Office manages the collation of publications containing scientific work resulting from the Australian Synchrotron beamlines.

In addition to the operations based in Australia, the User Office runs the International Synchrotron Access Program, which funds Australian research groups travelling overseas to other synchrotron facilities.

The main achievement of the period covered by this report was the successful management of over 4000 safe user visits to the Australian Synchrotron. The ongoing user exit survey reported that for this period, the average user felt their experience with the User Office was between "good" and "excellent".

Looking forward, the group will continue improving its processes to meet the demand of growing user numbers, which will see an increasing utilisation of web-based systems.

The User Office Team
Dr Cathy Harland, Group Leader, User Support
Ms Amanda Louch, User Office Administrator
Ms Eva Christopoulos, User Office Administrator

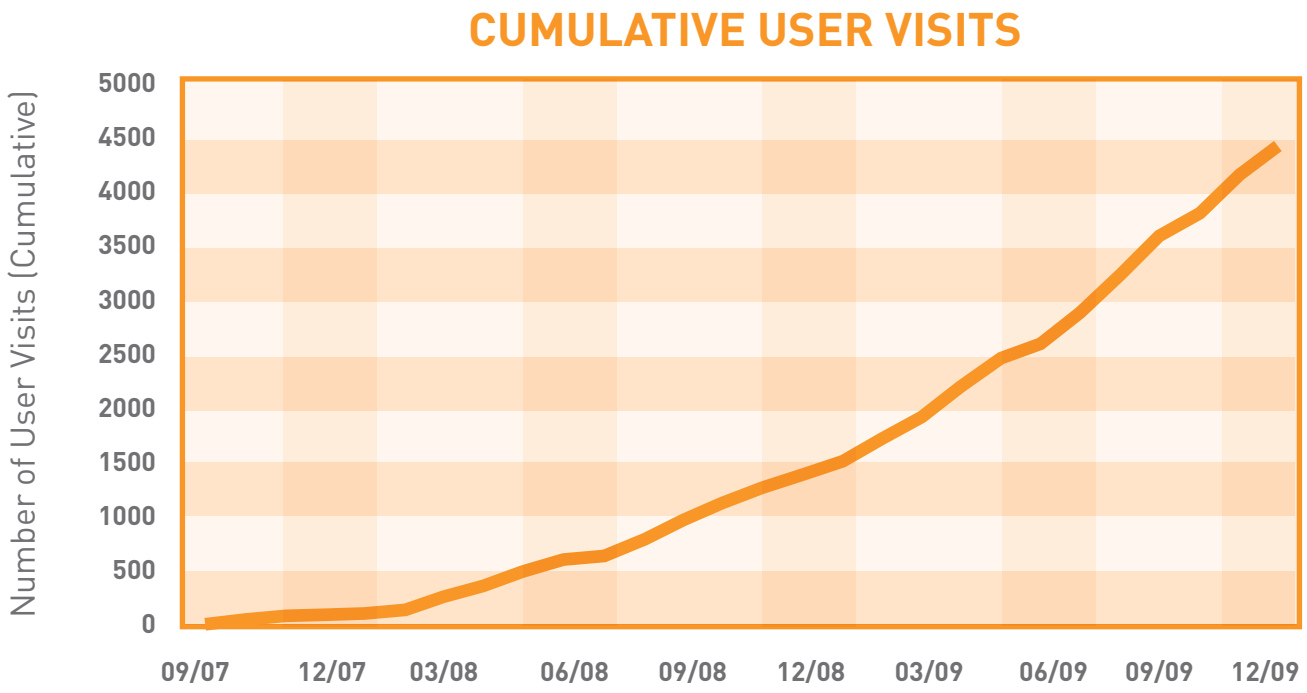

Australian Synchrotron Users

User access

The allocation of user access to the beamlines is based on the following schedule:

Merit-based (approximately 50 percent)

Merit beamtime is allocated through a competitive, peer review process. There are three open 'calls for proposals' each year which relate to three beamtime periods. Typically the call for proposals is open for one month, and closes two months ahead of the scheduling period. The first round is from January to May, the second round is from June to September, and the third is from September to December of each year.

Proposals received are reviewed for scientific merit and technical feasibility by a specialist committee. Users are notified of the result of their application within three weeks of the submission date.

Foundation Investor (approximately 30 percent)

Foundation Investor proposals are not subject to peer review and are allocated beamtime by the Foundation Investor Consortia subject to satisfactory safety and technical feasibility criteria. This arrangement remains in place for six years from the time of the first beamline becoming operational in September 2007.

Facility and commercial access (approximately 20 percent)

This includes access for scientists working at the Australian Synchrotron to further their own research projects. A commercial program is also in operation and has achieved significant revenue.

Applying for beamtime

To apply to use one or more of the facility's beamlines, a user needs to submit an application via the Australian Synchrotron's online proposal system. This can be done by visiting:
http://portal.synchrotron.org.au/<http://portal.synchrotron.org.au/AS/proposal/index.jsp>

User support

Users of the Australian Synchrotron are fully supported to ensure that they are able to make efficient use of their visit to the facility. Prior to visiting the facility the User Office manages interactions with users, assisting with the proposal process, accommodation booking and travel support. The Australian Synchrotron user experience while on site includes:

- Comprehensive safety and beamline induction training on arrival
- Extensive, hands-on support from our beamline scientists during business hours on all week-days
- Direct support and assistance from our beamline scientists with any trouble-shooting outside of business hours
- Support from our machine operators with common faults when beamline scientists are not available
- On-call support from beamline staff for any significant technical issues.

The Australian Synchrotron also provides extensive facilities to support our users in preparation and analysis of their samples, including laboratory space and equipment and post-experimental support and analysis to assist in the preparation of scientific papers.

Australian Synchrotron Users

Our user community

The Australian Synchrotron user community is growing and diverse. It includes a mix of government, academic and industrial scientists from all over Australia and New Zealand and the rest of the world. A number of our users are students and early-career researchers, indicating the important role of the Australian Synchrotron in the development of the national and international synchrotron science community.

Submitted proposals by location for 2007 - 2009

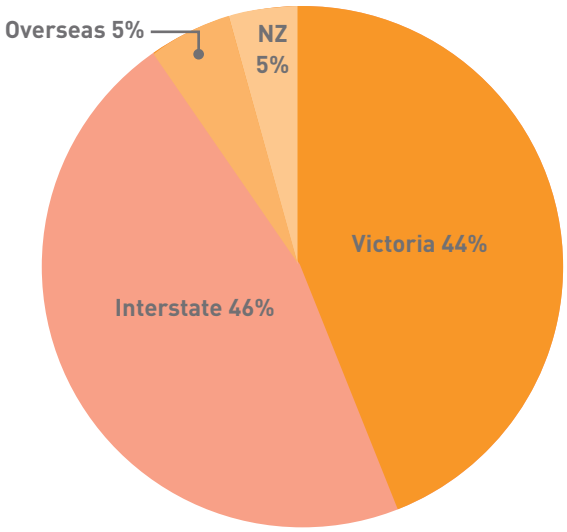

Submitted proposals by beamline for 2007 - 2009

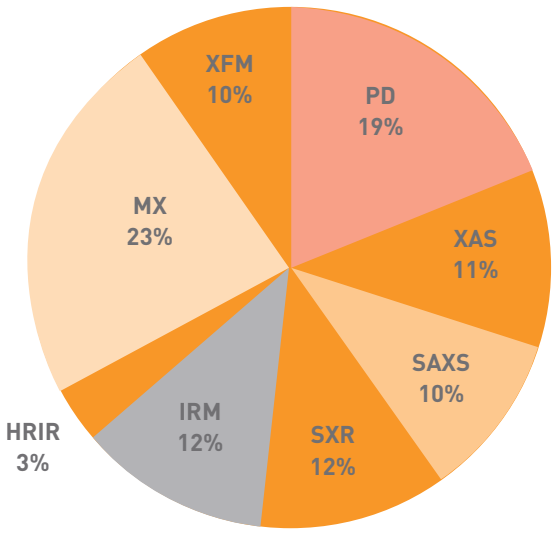

Australian Synchrotron Registered Users

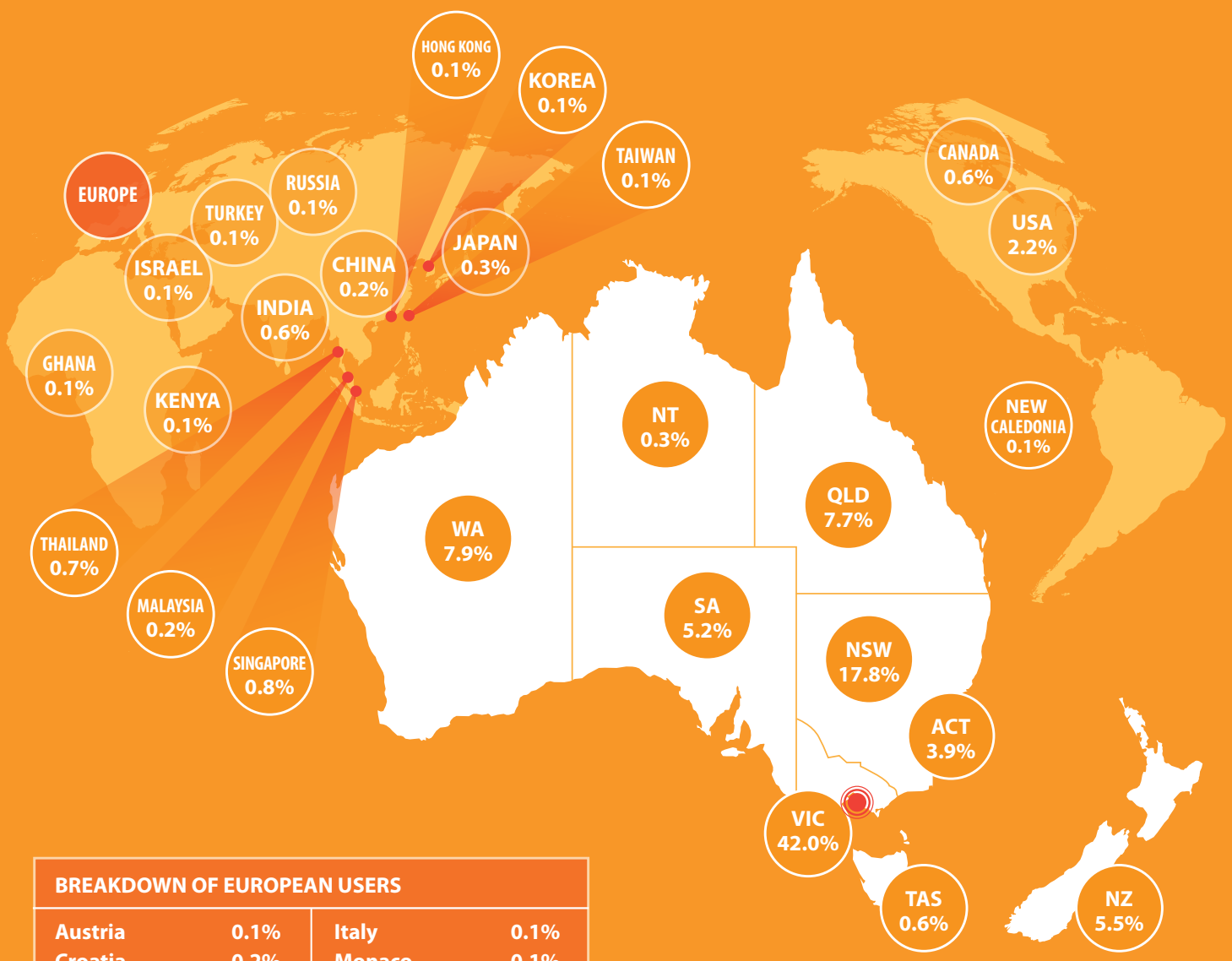

BREAKDOWN OF EUROPEAN USERS			
Austria	0.1%	Italy	0.1%
Croatia	0.2%	Monaco	0.1%
Demark	0.1%	Portugal	0.1%
Finland	0.1%	Slovakia	0.1%
France	0.6%	UK	0.9%
Germany	0.2%		

Note: 'Registered Users' include those Users that are registered on the Australian Synchrotron database.

Foundation Investors

The Australian Synchrotron was established as part of a partnership between the Victorian Government and the Australian Government.

Additional investment and support came from the New Zealand Government, other Australian state governments and six publicly funded research institutes, 33 universities, 37 medical research institutes from across New Zealand and Australia.

As Foundation Investors (FIs), these groups have played a critical role in the facility's development, with each contributing a minimum of $5 million to the establishment and operation of this world-class science and research facility. Each continues to play an active part in the Australian Synchrotron's governance as primary advisers to the Australian Synchrotron Board.

Supported by

Australian Government

State Government Victoria

Foundation Investors

AAMRI

ANSTO

CSIRO

Monash University

University of Melbourne

New Zealand Consortium

New Zealand Government

Victoria University of Wellington

University of Auckland

University of Otago

University of Canterbury

Crop Grains Science Limited

University of Waikato

Massey University

Lincoln University

IRL (Industrial Research Limited)

Agresearch

Foundation Investors

AUSyn14 Consortium

NSW Government

University of Western Sydney

University of New England

Southern Cross University

Charles Darwin University NT

Charles Sturt University

University of Technology Sydney

University of Canberra

University of NSW

University of Newcastle

University of Wollongong

University of Sydney

University of Tasmania

Macquarie University

Queensland Consortium

QLD Government

Griffith University

James Cook University

Queensland University of Technology

University of Queensland

South Australian and La Trobe Consortium

Government of South Australia

Flinders University

University of Adelaide

University of South Australia

La Trobe University

Western Australian Consortium

Government of Western Australia

University of Western Australia

Curtin University

Australian Synchrotron
800 Blackburn Road
Clayton, Victoria, Australia 3168
t. +61 3 8540 4100
f. +61 3 8540 4200

www.synchrotron.org.au